Effect of Graphene Nano Sheet On The Properties of Al-6061/B_4C Composites

By

Abdul Malik
(214-FBAS/MSPHY/F13)

DEPARTMENT OF PHYSICS
FACULTY OF BASIC & APPLIED SCIENCES
INTERNATIONAL ISLAMIC UNIVERSITY, ISLAMABAD

Session: (2013-2015)

Department of Physics
Faculty of Basic & Applied Sciences
International Islamic University, Islamabad, Pakistan

23.6.16

CHAIRMAN
DEPT. OF PHYSICS
International Islamic University
Islamabad

Chairman, Department of Physics

Dean, FBAS,

International Islamic University, Islamabad

Certificate of Approval

It is certified that the work presented in the thesis entitled **"Effect of Graphene Nano Sheet On The Properties of Al-6061/B_4C Composites"** by **Abdul Malik** bearing **Registration No. 214-FBAS/MSPHY/F13** is of sufficient standard in scope and quality for award of degree of MS Physics from International Islamic University, Islamabad.

COMMITTEE

External Examiner
Professor Dr. Ishaq Ahmed
Department of Physics
CIIT Islamabad

Internal Examiner
Dr. Wiqar Hussain Shah
Assistant Professor
Department of Physics, FBAS, IIUI

Supervisor:
Dr. Waqar Adil Syed
Associate Professor
Department of Physics, FBAS, IIUI

9-8-16

Co Supervisor:
Dr. Rafi-Ud-Din
Material Engineer
PINSTECH (PAEC)

20.08.2016

A Thesis submitted to

Department of Physics

International Islamic University Islamabad

As a partial fulfillment for the award of the degree of

MS Physics

FORWARDING SHEET BY RESEARCH SUPERVISOR

The dissertation entitled "**Effect of Graphene Nano Sheet On The Properties of Al-6061/B_4C Composites**" submitted by **Abdul Malik** in partial fulfilment of MS degree in Physics has been completed under my guidance and supervision. I am satisfied with the quality of student's research work and allow him to submit this thesis for further process to graduate with Master of Science degree from Department of Physics, as per IIU rules and regulations

Dr. Waqar Adil Syed,
Associate Professor
Department of Physics,
International Islamic University,
Islamabad

Dated: _____

Declaration of Originality

I hereby declare that the work contained in this thesis and the intellectual content of this thesis are the product of my own work. This thesis has not been previously published in any form nor does it contain any verbatim of the published resources which could be treated as infringement of the international copyright law.

I also declare that I do understand the terms 'copyright' and 'plagiarism,' and that in case of any copyright violation or plagiarism found in this work, I will be held fully responsible of the consequences of any such violation.

Signature: _____

Name: _____

Date: _____

Place: _____

Dedication

*"I dedicate this work to my loving **parents** who have always been the source of motivation in my every struggle of life"*

Acknowledgement

Upon the completion of this work, first of all, I owe a deep sense of gratitude to Allah (S.W.T.), the Almighty, to whom we all belong and to whom we turn in every moment of grief and joy. I am extremely thankful to the technical lab staff at Materials Division, PINSTECH for their support and guidance in carrying out the experiments.

I also feel indebted to my project supervisor, Dr. Waqar Adil Syed, and Co-Supervisor,Dr. Rafi-Ud-Din whose scholarly advice, meticulous scrutiny and professional directions refined and beautified my practical and written work. Their enthusiasm and effort in accomplishing this research is the main reason for its early enough completion.

Lastly, I would extend my gratitude to my parents, siblings and friends for their invaluable prayers and wishes that have always blessed me with success in all fields of life.

Abdul Malik

Table of Contents

List of Figures

List of Tables

Abstract

Graphene nanoplatelets were prepared with modified Hummer's method. Raman spectroscopy, SEM morphology and XRD analysis were employed to characterize graphene nanoplatelets. Raman spectroscopy results indicate that graphene was comprised of 5 layers of carbon. Subsequently, Aluminum-6061 alloy reinforced with 4 vol % B_4C composite were prepared by powder metallurgy route. Further the effects of graphene addition on Al-6061/B_4C composites were investigated in detail. The resulting Al-6061/B_4C composites with graphene additions were characterized by (SEM) and (XRD) analysis. XRD results validated the presence of B_4C and graphene in the Al-6061/B_4C/graphene hybrid composites. The results indicated that density and hardness had increased with graphene additions to composites. Additionally there was no interfacial reaction product observed between the reinforcements and aluminium matrix as observed by XRD analysis.

1. Introduction

1.1 Metal Matrix Composites

Composites are composed of two or more different materials to obtain a combination of properties not available in either of the material. MMCs are Metal Matrix composites while PMCs are Polymer matrix composites, which are very popular. MMCs are the broad family of the materials in contrast to PMCs. These innovative materials are fabricated and analyzed since 1980 [1]. MMCs are superior to an unreinforced metal. It consists of two different constituent parts; the base metal alloy (matrix) and reinforced material (filler). Cermet's consist of ceramic and metal, it has combination of properties, such as hardness and plastic deformation corresponding to ceramic and metal. Hybrid materials consist of two reinforcement materials; it can be ceramic, metal or an organic compound [2].Hybrid materials are the major interest of the researchers. Combined behavior of the hybrid composite consistsof the volume and the chemical stability of each individual used during fabrication. The main feature is favorable balance between inherent advantages and disadvantages [3]. Many researchers termed them as, Light weight metal matrix composites, because the constituents used have low densities and lightweight materials [4]. These composites at nano scale are different from the traditional materials in which the constituents are macroscopic (Micro to millimeter). MMCs produced via different routes consist of primary objective to improve the mechanical properties with low density, so for the researchers have main concerned with lighter structural metals or allcy. Moreover the number of research papers has been published to achieve the better combination of, corrosion properties, wear properties, thermal properties, electrical properties, and mechanical properties [5].

MMCs are better than poly matrix composites (PMC) at higher temperature. The production of MMCs is little tough and expensive, However the technology is in competition with other branches of Physics and playing an important role in the development of materials. The matrix is usually a monolithic material in a large quantity and purely continuous; one can embed the reinforced materials which are purely discontinuous. MMCs are made by dispersion of ceramic or any metal reinforced into the matrix. The big task till now is to prevent the interfacial reaction in composites [6]. The reinforced material doesn't always provide structural task, instead of this it is used to enhance the mechanical properties, electrical properties as well as thermal conductivity

[7]. These innovative materials, including ceramic and non-metals open up countless possibilities in hybrid composites. The characteristics and fabrication of metal matrix composites depend upon the shape and their size. So the suitable volume of reinforced material, MMCs obtained the desired and conceptual outcome of researchers. There are some other preconditioned objectives, such as strength of conducting materials, and wear properties, while maintaining the high conductivity. The more concentrated area is the production of ductile composites and magnetic materials with extremely low density. Many base metals as matrix has been used including magnesium, iron, steel, copper, carbon and aluminium [13]. Figure 1-1 shows that metal matrix composites are only at the beginning of the evolution curve of modern materials, and it also illustrate the comparison of aluminium with other metals.

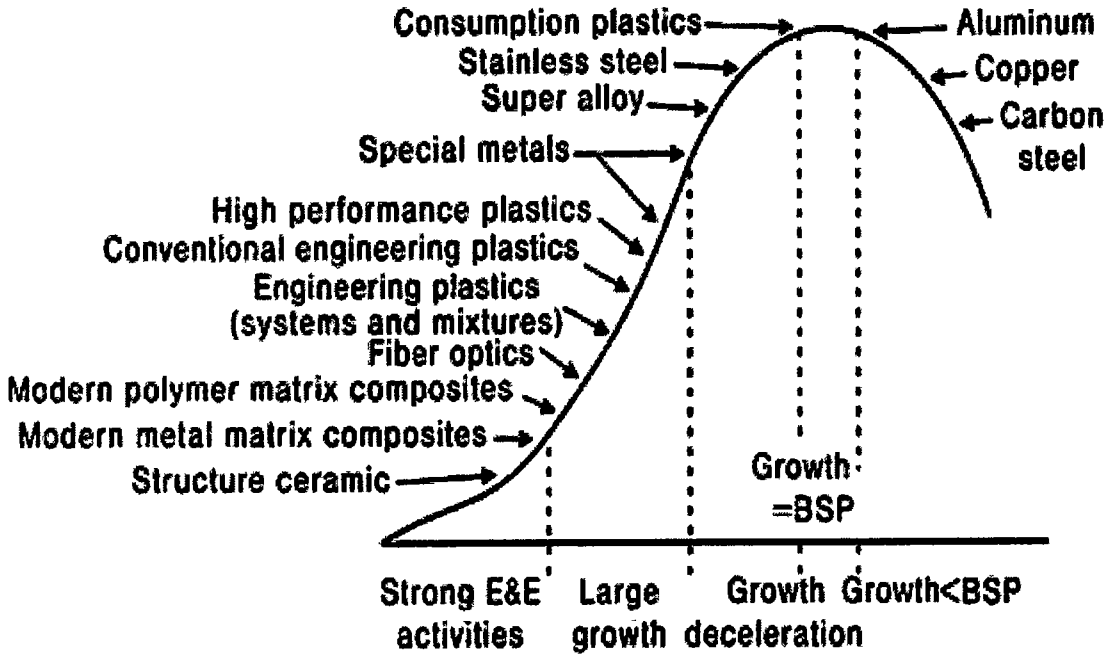

Figure 1-1: Comparison of aluminium matrix with other matrix

Each of them has its own application and properties in their respective areas, but among them aluminium is a remarkable base metal matrix for the production of conceptual outcomes.There are a lot of application of MMCs such as fan blades, aerospace, automotive, aircraft brake pad, oil less bearing, magnetic disks and aeronautical etc. [8] The first application for particle reinforced MMC in united states was set of covers for missile guiding system.As there are a lot of advantages and applications of MMCs, but there are some disadvantages compared with metals. Primary of them is high amount of cost for fabrication of high performance, low toughness, and loss in ductility.

To summarize the specific weight and improvement in properties can find many application areas. So, currently it has considerable applications in military industry and aerospace.

1.2 Aluminium Matrix Composites (AMCs)

During last decades, tremendous progress has been made in the field of composites with reinforcement of specific metal or ceramic particles. Many base materials (Matrix) have been used; depending upon the choice of the application. As mentioned before metal matrix generally used are magnesium, steel, titanium, iron etc., but aluminium with atomic number 13, has been widely used as a metal matrix for metal matrix composites. Steel is heavier than aluminium (density ~7.8 g/cm^3). Similarly, magnesium is more expensive, so it is very costly to use as a structural material.Until nowthe interesting base matrix metal is aluminium with the feature of low density ~ 2.71 g/cm^3 and high ductility. It is more strengthened and lighter weight metal rather than any other metal. Aluminium is third abundant material found in the earth's crust after oxygen and silicon, so this is cheaper than any other competitor. The pure aluminium does not have favorable properties in competition with aluminium alloys. Figure 1-2 shows the pure aluminium and aluminium alloy.

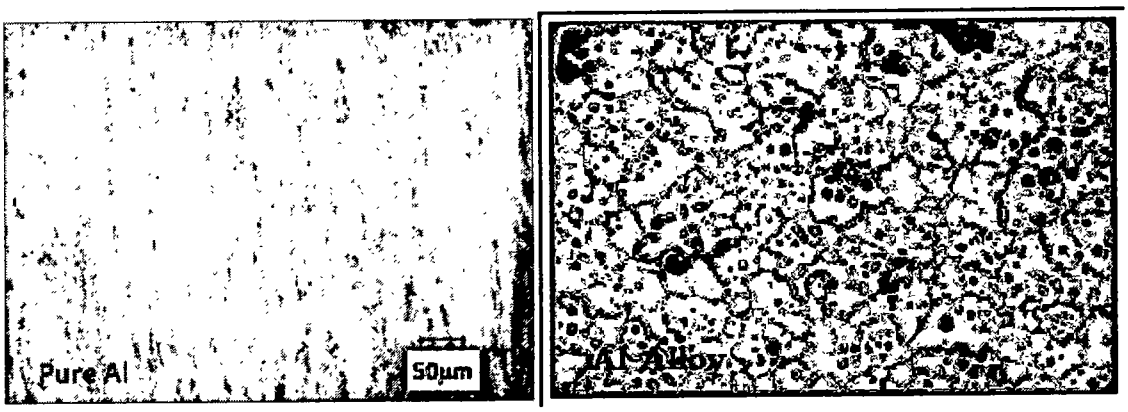

Figure 1-2: Microscopic view of Pure Aluminium (left) and Aluminium Alloy (right)

Aluminium alloy composition depends upon, different percentages of various elements, including, magnesium, copper, manganese, silicon and tin, etc. as shown in Table: 3-1. Some useful alloys are Al-6061, Al-7075, Al-7068, Al-5052, andAl-2024. Each of the alloys has its own properties and the dimensions, but among them, Al-6061 has better properties i.e., it has a high strength to weight ratio, high stiffened alloy,lower thermal expansion coefficient, higher resistance to thermal fatigue and creep, corrosion resistance, fluidity and castability [9, 10, 11]. Moreover it has high ductility than monolithic alloy. Al-6061 facilitates the fabrication process and put no barrier for the complexity of the

material that can be fabricated Monolithic form of aluminium does not have more favorable results in comparison with aluminium reinforced by any metal or ceramic material and it was also observe that aluminium is poor resistant to wear [12].

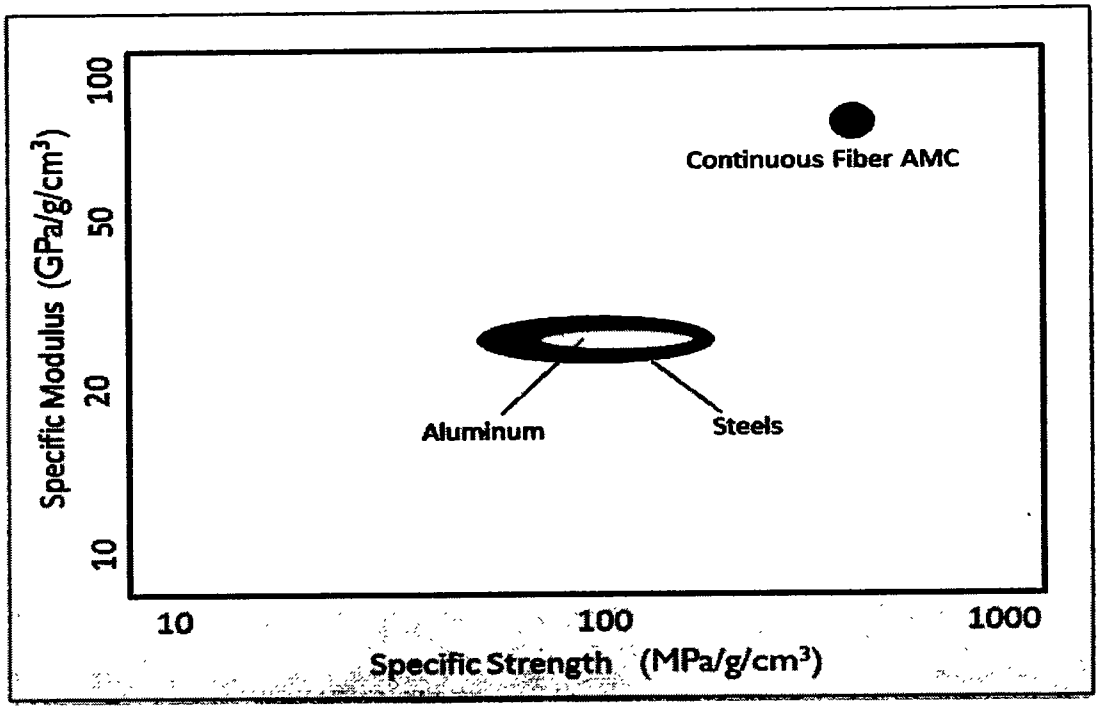

Figure 1-3: Graphical comparison of the mechanical properties between continuous fiber reinforced AMCs and steels.

Aluminium alloy generally reinforced with Al_2O_3, SiC, C, SiO_2, B, BN, B_4C and CNT. Hartaj Singh et al, have suggested many techniques for the development of metal matrix composites by reinforcing ceramic particulates as well as by fibers. The aluminium reinforced with CNT has been a wide interest of the researchers. They have made contribution in MMC production reinforced with graphite and CNT. For reinforcement of CNT and graphene, tensile strength for CNT reinforced composite was approximately 12% increase in comparison with monolithic aluminium. While the graphene as reinforcement showed 18% less tensile strength [13]. The strength of aluminium matrix composites can be analyzed with the fact that, aluminium reinforced with SiC, results in high stiffness 67% like cast iron, whereas continuous fiber reinforced in aluminium matrix produces high stiffness as well as high strength like steel as shown in Figure 1-3.

1.3 Types of Reinforcements for AMCs

Reinforcement also known as filler, used to make MMCs more productive in various reasonable applications. Low densities, with good mechanical and electrical properties are the general demands that are required. During the last decade, researchers have used many reinforcement types like, mono filaments, whiskers/short fibers, long fibers and particles. Owing to high density metallic fibers are failed. Among them reinforced material via particle is more attractive.

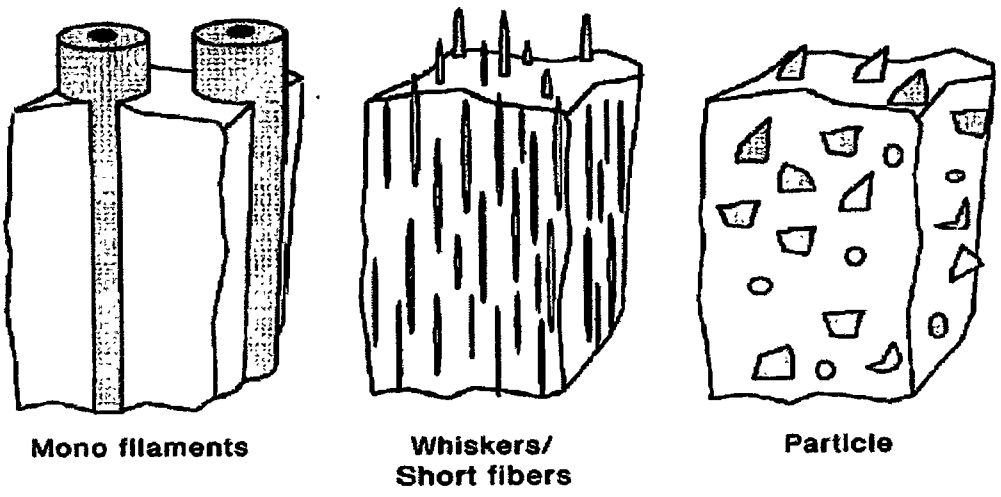

Figure 1-4: Schematic diagrams of composites reinforced with monofilaments, whiskers and particles

As aluminium is a vast using metal matrix, so a wide range of suitablepotential reinforced materials for aluminium matrix are used, including SiC, B_3N_4, graphene, graphite, Al_2O_3, ZrO_2, TiB_2 and B_4C and CNT. These reinforced materials exist in the form of, mono filaments, short fibers/whiskers, long fibers, and particles. Each of the reinforcement type has a typical profile, which is responsible for the effect in the composites for superior mechanical properties. For couple of years a lot of work has been published for Al-6061 reinforced with SiC, Al_2O_3 and CNT for the production of MMCs. A schematic diagram of reinforced monofilament, whiskers/short fibers and particle is shown in Figure 1-4.

1.3.1 Boron Carbide as reinforcement

Boron carbide is a ceramic materialhas been used as an attractive reinforcement to obtain primary objective, low density and light weight composites. Precisely B_4C is one of the better reinforced materials with melting point ~ 2450°C, and lower density 2.53 g/cm^3. B_4C is a good reinforcement for aluminum matrix due to the several unique physical properties. After diamond Boron carbide is 3rd hardest ceramic material, with greater

thermal and mechanical properties like chemical stability comparable to SiC and Al_2O_3. Further it is unique due to high shock resistance and high wear resistance [14].

There are two isotopes of Boron, ^{11}B (80.1%) and ^{10}B (19.9%), neutron capture cross section for Boron-10 isotope is 3840 barns while that for Boron-11 is 5 barns.^{10}B isotope has a greater cross section;so the material is used in the nuclear field as control road fixture, that's why B_4C is also a neutron absorber. The characteristic of neutron absorption has made B_4C as a very preciousmaterial in material sciences. This ability leads B_4C to the main interest of the researchers.

Due to high reactivity of boron it is difficult to obtain pure boron, which is further complicated that impurities are present in the crystal lattice of boron and combined with any matrix.

1.3.2 Graphene as reinforcement

With advancement in technology the most innovative material graphene was introduced in 2004 by A. K Geim and K. S Novoselov [15]. Graphene is Sp2 hybridized two dimensionally hexagonal honeycomb structures which depend upon the single layer carbon atoms. The strongest and stiffest material ever measured with the property of stretchable crystal after diamond. So far graphene has been in the interest of the researchers; many publications during the last decades have been published with the name of graphene as shown in Figure 1-5.

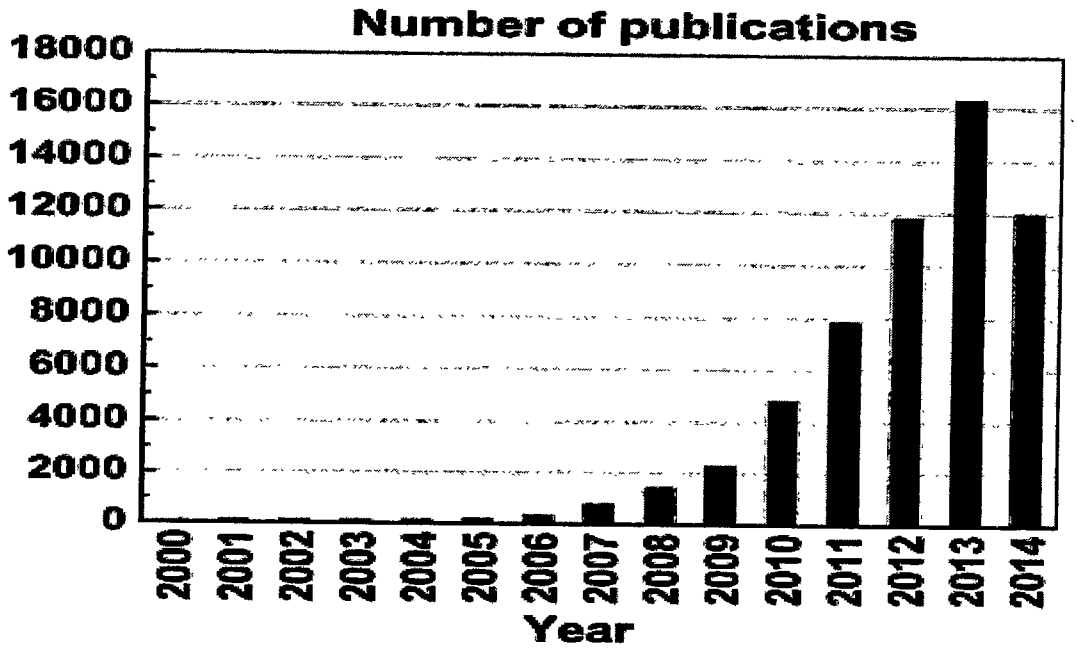

Figure 1-5: The Number of paper published at graphene in each year.

Graphene is solid lubricant because of its favorable conditions of chemical inertness and low friction, and it also has a capability of film forming on metal surfaces. It is considered to promote the relative motion and arrangements of the particles in the matrix which results in higher density of the composites. According to Web of Science database, there were 164 papers were published with the word "Graphene" in 2004. A total of 3,671 papers were published in 2010 according to Thomson Routers Web of knowledge. Figure 1-5: shows the number of publications on word graphene from 2000 to 2014.

1.3.3 Silicon Carbide (SiC) as reinforcement

Silicon carbide reinforced material also produced a tremendous progress in AMCs. Silicon carbide as a reinforcement improve both strength and wear resistance of composites at 20% volume of SiC, but an increase in volume of SiC leads to the brittleness in the composites. Furthermore large porosity was observed in composites of SiC. The mechanical properties are increased due to the SiC particles in composites. The problem may arise when SiC reinforced in aluminium matrix, may react with inter phases and produce Al_4C_3.In literature it was found that, during short time sintering the formation of the Al_4C_3 was not observed. During Plastic deformation in powder metallurgy, the uniform distributed SiC particles provided an advantage to bear the load that exerted to check the hardness of the material. Therefore, it was observed that, this material offers fruitful production in applications, with good thermal and tensile properties. Comparison of B_4C and SiC provided,B_4C is much better reinforcement used by researchers as it produces greater thermal and mechanical properties, with low porosity and extremely high hardness.

1.3.4 Carbon Nano Tube (CNT) as reinforcement

Carbon nano tube are formed by Chemical vapor deposition, which is also effective reinforcement material used during last couple of years. It also has low density with respect to graphene and other reinforced materials. The uniform distribution of CNTs in matrix is a big problem as it is inhomogeneous in Mg matrix [16]. Consequently uniform distribution was remained the major challenge for the CNT. Powder metallurgy was used to attain the uniform distribution (homogeneously) of the particle which produces good result rather than stir casting technique.

Zhan et al. reported uniform distribution problem or CNT reinforced in aluminium matrix composites was not a big issue. As aluminum have greater plasticity, so CNT surface were mixed with aluminium powder [17].

Fan et al. observed a 100% improvement in fracture toughness with and 20% in flexural strength with the addition of only 1 wt.-% SWNTs.However they observed uniform distribution as well as small amount of agglomeration in 6061-Al/CNT composites. The phenomenon of agglomeration produced during the mixing was caused by the Vander walls forces between the particles [18].

1.4 Aluminium – Boron Carbide Composites

Of the reinforced material mentioned above B_4C is more attractive in this class. It is a ceramic material as well as more brittle than aluminium. According to web of encyclopedia, B_4C has a much greater tensile strength of 270 MPa and young modulus of 470 GPa in comparison with aluminium 2700MPa and 75 GPa respectively. This large variance in modulus of B_4C produced stiffness in the composite, but the key point is uniform distribution. Most B_4C particle reinforcements range from 0.5 to 100 μm, a strong interface between 6061-Al and B_4C required during fabrication. Uniformly distributed B_4C particles carry the load in composites.For MMCs two materials are constrained and must strain to the same level, caused a shear force on the B_4C that transfers the load from the matrix to the ceramic.

Until now Limited research has been conducted, due to the high cost of the material. Aluminium reinforced with boron carbide composite become very attractive, especially inthe manufacturing of MMCs as well as in neutron absorption application. This composite is used as shielding materials to absorb free neutrons, produced from the reaction in the nuclear reactor and to avoid any radiation escape to the surrounding environment.

In contrast with Aluminium, Boron carbide also has low density 2.53 g/cm^3 that suggest a good machinability between B_4C (filler) and aluminium (matrix).Aluminium has higher density which is approximately 2.70 g/cm^3 compared to boron carbide,so the combination of these two materials will produce a composite with lower density. As mention above that the tensile strength is 3.7 times higher than aluminium, whereas the elastic modulus is 4 times higher, these parameters are suitable for aluminium to make better MMCs.

Table 1-1: The comparison of the properties between Boron carbide and Aluminium

Property	Aluminium	Boron Carbide
Crystal Structure	FCC	Rhombohedral
Melting point (°C)	660	2760
Density (g/cm3)	2.71	2.52
Tensile strength (MPa)	150	560
Elastic Modulus (GPa)	69	270
Coefficient of thermal expansion ($\times 10^{-6}$ K^{-1})	23	3.2

Ehsan *et al.* investigated micro structural and mechanical properties of Al/B_4C composite [19]. With three variations in composition and four variations in sintering temperatures, and using microwave heating, they studied the effect of increasing B_4C content on the microstructure and mechanical properties of the composite. Their experiments showed that both micro hardness and compressive strength increased with increasing B_4C content.

B. Manjunatha *et al.* investigated the effect of mechanical and thermal loading on B_4C reinforced 6061 alloy [20]. They showed that both extrusion and heat treatment (mechanical and thermal treatments) have increased ultimate tensile strength and hardness of the composite. However, the increase in these properties from thermal loading was less than that from extrusion.

Z. Asghar *et al.* reported the effect of degassing parameters on sinterability of Al-B_4C powder mixture [21]. Three variations in degassing environment coupled with two variations in the sintering environment were investigated for a fixed composition. They found that samples degassed under vacuum and sintered in nitrogen atmosphere showed highest density.

Y. Abdullah *et al.* investigated the preparation, physical and mechanical properties of Al/B_4C composite with two variations in the composition of the powder [22]. They

found an increase in density with increasing milling times from 8 hours to 16 hours.

M. Khakbiz and F. Akhlaghi synthesized Al/B_4C nano-composite powders by mechanical alloying [23]. Mohanty, with some others, investigated the phases that are formed after vacuum sintering at 600^{o}C in Al/B_4C composite system. They found that with an increase of boron carbide content, there was a transition from Al/B/C formation to formation of boron rich Al-B at the grain boundaries [24].

C. Z. Nie *et al.* investigated the microstructure evolution of Al-B_4C composite during mechanicalalloying and the mechanical properties of the composite prepared by mechanical alloying-hot extrusion technique [25].

Sharifi et al. also investigated mechanical properties of AMCs reinforced with B_4C. He found that, by increasing the milling time up to 5 hours results in the form of uniform distribution, after 5 hours of milling uneven distribution was observed.He observed that the increased in B_4C composition, results in decrease in the density of the Al/B_4C composites, while wear resistance increased with increase in amount of B_4C. He also studied the effect of AMCs hardness with optimization of milling time up to 45 hours. The hardness was increased with milling time. The hardness sufficiently increased in early milling process, but the rate of hardness decrease after 5 hours. He also observed that the increase in hardness depends on both the strain of grain result from PM process and from uniform distribution of the B_4C nano particles [26].

Mohanty et al. (2008) in his study of fabrication technique and characterization of Al/B_4C composites also determined that the increased in volume of B_4C results decrease in the density of the metal matrix composite. He fabricated composite reinforced with 0-25% volume of B_4C and observed that the density of composite material decreased from 2.52 g/cm^3 to 1.8 g/cm^3. Furthermore, he also stated that the density of composite decreases as it shows increasing amount of porosities [27].

Kerti and Topan, 2008 and Toptan et al., 2010 also showed that B_4C as reinforcement took more attention especially with low cost casting routes [28]. Mixing conditions for Al-B_4C composite system have been studied very rarely. Different mixing parameters when considering ball mill include type of mixer, mixing mode (wet or dry), mixing time, revolution speed of ball mill and ball to charge ratio. Optimization of these parameters is

essential for qualifying efficient mixing procedures. An efficient mixing procedure will not only ensure good dispersion of the reinforcement (filler) in the matrix but it will also be efficient in the utilization of resources and energy.

B_4C is more brittle than aluminium. Introducing B_4C particles, the strength of the MMCs will increase with increase in volume of B_4C which leads to decrease in ductility and produced flexural strength. Instead of a loss in ductility, Aluminium reinforced with B_4C has more favorable results in MMCs; the most reasonable is high strength, low density of MMCs and extremely high hardness comparable with Al_2O_3 and SiC. [29]. It also produced greater wear resistance rather than monolithic aluminium metal. The studies reveals the fact, an increase in B_4C content in the matrix will increase the strength of the material, but main disadvantage is porosity and density which increased with the increase in percentage amount of B_4C. It is due to the agglomeration of the B4C particle in the MMCs. Porosities in the composites are very attractive for electrical properties but it deteriorates the strength of the material.

In literature it was found that the hardness of AMCs reinforced with 10% vol. of B_4C composites is greater than 5% vol. B_4C. The difference of the B_4C volume in the composite leads to the hardness value. B_4C has a higher strength compared with aluminum the ration of B_4C to aluminium is (2.75Mohs: 9.3Mohs). This yields that the increase in the % vol. of B_4C, increases the strength of the Al/B_4C composites. These all result also supported by report from Sharifi et al [24]. Other applications for boron carbide reinforced AMCs are substrates for computer hard disks and armor plate materials. Figure 1-6 shows a B_4C uniform distribution in an aluminum matrix as well difference between particle reinforcement and fiber reinforcement.

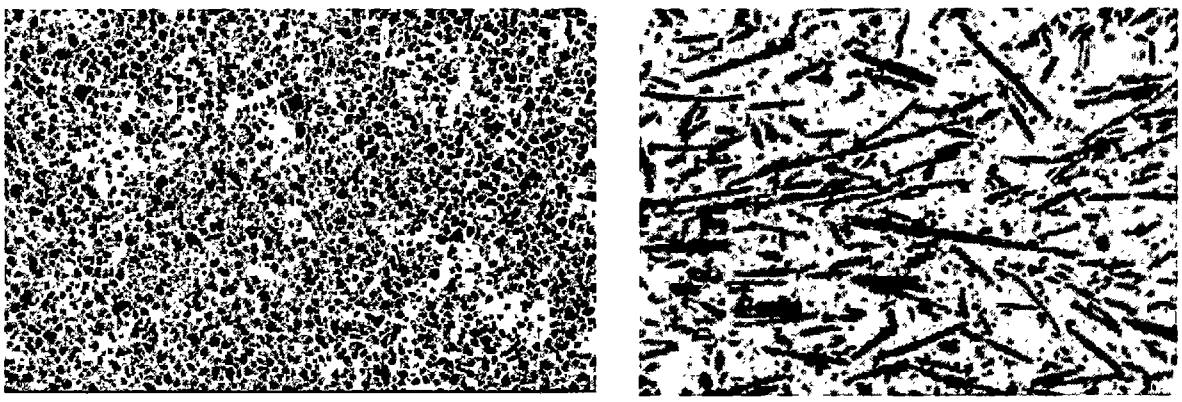

Figure 1-6: Micrographs of (a) particle-reinforced Al/B4C metal matrix composite, and (b) short fiber-reinforced Al/Al_2O_3 metal matrix composite

1.5 Aluminium – Graphene Composites

Graphene is a solid lubricant in which carbon atoms are arranged in the form of layers. When slide it on any other surface, it provides a very low coefficient of friction and due to the versatility researchers termed it as a solid lubricant. As we know that aluminium is poor resistance to wear, on other hand graphene is the solid lubricant and have better resistance to wear so, aluminium reinforced graphene have good impact on wear resistance with excellent mechanical compatibility. The addition of an appropriate percentage of graphene can lead to reduced wear rates of aluminium matrix composites as well as the strength of the material increased with the increase percentage of the graphene in MMCs. The addition of graphene also has a drawback; it will lead to a reduction of hardness and flexural strength [30].

In metal matrix composites the dislocation density depends upon the reinforced particles and their ranges, the greater dislocation density results in the greater strength of the composite. Owing to attractive property of solid lubricant of graphene it is used in many applications such as sensors, ultra-capacitors, and solar cells etc.

Graphene has many novel properties, but the main problem is dispersion of graphene in aluminium matrix due to high surface area to volume ratio. Most of the data published in MMCs reinforced with graphene deals with tensile properties, contrary less amounts of data available on compression strength. Aluminium reinforced with graphene with various percentages of 0.5%, 1 % and 1.5 %, are present. Above 1.0wt% of graphene nano flakes produces strengthening effect, which was sharply dropped due to the clustering of graphene nano flakes.However, the formation of carbides above 600 °C was reported by some publications which provide a useful mixing of aluminium with graphene particles during powder metallurgy process. Wang with his co-workers utilized the novel approach of flake powder metallurgy to produce 6061-Al/graphene composites, with dramatic enhancement in strength as compared to monolithic alloy [33].

Awerbuch et al. stated that, if L/D ratio is equal to unity, then deformation could be more than 50%. Such effects could also be responsible for high value of the compressive strength of material [31].

Khalid et al. developed 6061-Al/graphene composites by using liquid metal infiltration, where composites show good interfacial bonding between matrix and fullerenes. But

mechanical properties were less compared to theoretical calculation of superior stiffness/strength of fullerenes [32].The important physical and mechanical properties of graphene are mentioned in Table 1-2.

Table 2-1: Important Physical and Mechanical Properties of Graphene

Characteristics	Graphene
Electron mobility	1500 cm2 V^{-1} s^{-1}
Resistivity	10-6Ω-cm
Thermal conductivity	5.3 ×103 Wm^{-1} K^{-1}
Transmittance	>95% for 2nm thick film >70% for 10nm thick film
Elastic modulus	0.5 to 1.00 TPa
Coefficient of thermal expansion	-6×10^{-4}/K
Elastic modulus	0.5 – 1 TPa
Specific Surface area	2630m^2 g^{-1}
Tensile strength	130 GPa

1.6 Processing of Aluminium Matrix Composites

Hybrid composites have attracted great attention since 1980 [1]. For the production of metal matrix composites, the researchers designed many methodologies and techniques. Generally fabrication is carried out with two methods, liquid state and solid state methods. Stir casting technique is Liquid state, while solid state is powder metallurgy. Stir casting technique is an old technique, in which reinforcement in molten form is mix with matrix to produce the composites. But the main problem of stir casting is poor wettability during the mixing of ceramic material with matrix. However later modifications were made for controlling poor wettability but it remained a major issue. It was found that the MMCs fabricated by stir casting method suffers from particle pushing, results in the agglomeration and clustering of the particles at solid/liquid interface during powder solidification, Which was the main cause of decreasing the tensile properties as well as the ductility of the final composite by producing cracks in the composite [33]. Besides that many research papers has been published on fabrication and characterization of MMCs through stir casting, which have produced efficient results related mechanical properties of the composites. However, the key to obtain high ductility and tensile

strength, the dispersion of reinforced particles are fixed in grain interior rather them having agglomerated and clustering at the grain boundaries remained an issue in stir casting technique. [34-35].

Powder metallurgy is the best technique, experiencing a rapid developing period in the application rather than Liquid stir casting, because of loss of the material in stir casting and advantage to save on material in powder metallurgy [36]. In powder metallurgy special alloy at nano scale rather than micro scale are used for fast solidification during the composite production. Ceramic material can easily be used as reinforcement as it does not have poor wettability. Other advantages are better dimensional tolerances and lesser energy utilization per kilogram of the components andlesser requirement for post fabrication steps.

Maximum raw material utilization is the key point of powder metallurgy. As well as, powder metallurgy has some disadvantages such as the production of powder form of the material is not an easy task. The cost of die used for pellets is very high, limitations occur when dealing with a large production. Nevertheless, for small components powder metallurgy is the best method, and in return of high strength material, one can happily pay a high amount for die.

The main problem of the powder metallurgy is also the dispersion as the fine powder in nano scale of reinforcement is difficult to disperse in the matrix. Many methods have been developed to reach the goal, such as mechanical mixing, high-energy ball milling, solution assisted dispersion, and so on. The solution of the dispersion problem will lead the MMCs for vast utilization in the material field.

1.7 Significance of Reinforcement Distribution and Mixing

Nowadays, an increase in hardness is required in several applications. For the achievement of greater strength of aluminium alloys, it seems very difficult with conventional fabrication techniques. So, some novel approaches are required for mechanical properties of aluminium composites. Over some years two methods of nano crystallization are being employed for the effective production of the MMCs. First one is defined by the well-known Hall–Petch relationship [37, 38]. Second method is bulk nano-crystalline aluminium alloys (BNAs). These two methods exhibit a significant strength increase over monolithic aluminium. Generally, the fabrication of MMCs has been

divided into liquid state and solid state method. As stated earlier that solid state method is known as powder metallurgy (PM) method, which is experiencing a rapid developing period in application. With PM methods, the dispersion of nano or sub-micron reinforcements, the control of interface below the melting point of the matrix, and the precision forming of MMCs became possible, which promises a wide prospect for MMCs [39, 40].

Suresha et al. in 2010 have studied that certain suitable methods for MMCs are powder metallurgy, spray atomization and co-deposition, plasma spraying, stir casting and squeeze casting. Moreover, it also seems that the use of a single reinforcement in analuminiummatrix may sometimes compromise the values of its mechanical and tribological properties [41]. In powder metallurgy consolidation of powder, requires some process consisting of powder compacting (e.g., cold pressing, hot pressing, isostatic pressing, etc.), sintering (e.g., heating, spark plasma sintering, etc.) and deformation processing (e.g., extrusion, rolling, forging, etc.). These steps are enough for determine the relative density and structure of the bulk material, and influence the composite material properties directly [42].

By altering the manufacturing methodology and keeping the same reinforced material, one can obtain a different characteristic profiles. The characteristics of the MMCs are determined by their internal interfaces, grain interior and microstructures, while microstructure depends on the structure of the matrix and structure of reinforced material, and affected by their production and their pre-properties. Grain and sub grain size, texture and lattice defects are important parameters to the matrix for chemical composition of 1^{st} phase (Matrix), contrary for the 2^{nd} phase (Reinforced material) the grain size, volume, distribution and its kind are important factors. For example a large volume of B_4C reinforced in 6061-Al, the strength increases, but the ductility decreases. For using Al/B_4C composites as neutron shields, an efficient volume of B_4C and dispersion in the aluminium matrix will ensure uniform neutron shielding properties. Other properties that would be affected by reinforcement distribution are heat rejection capability and impact strength. An inefficient or segregated dispersion of boron carbide will not only affect the neutron absorption capability, but it will also lead to early crack initiation at the site of segregation [20].

For effective production, two parameters are very important for both types of methodologies, the first is homogeneous distribution of the particle in MMCs, while the second is the degree of adhesion or bonding of reinforced particles with metal matrix

phase. Degree of homogeneity depends upon the mixing of the two powders while the quality of adherence depends upon the chemical reaction between matrix and reinforcement. In powder metallurgy the mixing of the powder is carried out with ball mill, therefore optimization of time for ball milling is very important for homogenous dispersion. For various applications, homogeneity in strength, creep and corrosion resistance, electrical and thermal properties and density are some fundamental requirements.

1.8 Aluminium- Boron Carbide – Graphene Composites

During recent years graphite is used as reinforcement with Boron carbide for wear behavior and tensile properties. This approach is advantageous because of the better tribological applications as the graphite increases the resistance to seizure and improves the malleability of the matrix [43]. The methodology adopted was stir casting. As it is stated earlier that, aluminium reinforced with ceramic material produces higher tensile strength but also results in loss of ductility. For the purposes graphite particle were used to enhance the ductility and tensile properties as well as wear resistance of the composite. Wear is the system dependent property, and wear properties depend upon load, sliding speed, grain size, materials parameters and hardness. Substitution of graphite with graphene is also very promising as graphene has excellent mechanical properties.

Recently in 2014 the Zoltán Károly and Csaba Balázsi published a paper on hybrid composites via spark plasma sintering. The reinforcement was used are silicon carbide and graphite. They have concluded that an increasing the reinforcing phases increase the porosity decreases the hardness. Therefore, it is reasonable to avoid the incorporation of reinforcing particles. Because at higher amounts of filler in the matrix increased the incorporation of particles or their surface must be deposited previously with a thin film, which created good wetability to aluminium. In literature researcher also focused on aluminum alloy reinforced with SiC and B_4C, and they have also showed that mechanical properties increase with increasing amount of two ceramic reinforced materials. The methodology adopted was stir casting, which produces agglomeration, caused porosities in composites, which leads loss in strength. Still there is no research work found regarding aluminium reinforced with B_4C and graphene synthesized by powder metallurgy.

1.9 Motivation

Flexural strength, low density and low ductility of Al-6061 reinforced with B_4C particles are the major issues. Perhaps by increasing the B_4C content result in an increased in strength, but ductility of the composites has been decreased. Consequently to maintain the ductility of final composite to high, we have used two reinforced materials, Boron carbide and graphene particles. This work is an investigation of the mechanical properties of aluminium reinforced with B_4C and graphene composites prepared by solid state powder metallurgy. Production of Graphene was done via modified Hummer's method with suitable modifications and compared results obtained from SEM, Raman spectroscopy and XRD to those of previous work. Scanning electron microscopy (SEM), Raman spectroscopy, green density and X ray diffraction(XRD) analysis are studied for graphene and after each parameter of powder metallurgy e.g. Ball milling, compacting and sintering.

During this work particular attention has been focused to obtain uniform distribution, low green density, better flexural strength and mechanical properties of the hybrid composites in contrast with previous work.

2. Characterization Techniques

2.1 Scanning Electron Microscopy

(SEM) stands for Scanning Electron Microscopy, which is the type of electron microscope, used to produce images of a sample at micro or nano scale with the help of focused scanning beam of electrons. The beams of electrons are generated by electron gun. Electrons, bombarded at the sample, interact with it and produced signals that contain information related to the surface's topography of the material, and its composition. SEM can obtain an image of size approximately to 1 nm of a sample. The most common used of the SEM is the detection of secondary electron. These secondary electrons are generated during the interaction of the electrons with the molecules or atoms of the specimen. Number of secondary electrons that can be detected depends upon the contact angle of the bombarded beam of the electron with the sample. Scanning of the sample and by collecting of secondary electronwith the help of detector,an image can be display. [44] The SEM instrument usually consists upon two main components, electron column and electronic console. The electronic console provides switches and control knobs, for adjustment of the instrument features like filament currents, accelerating voltage, contrast, brightness and focus. All of these parameters are controlled with the help of computer system by using keyboard and mouse. User must be familiar with GUI programs, and modern software's to run and control the parameters rather than controlling them typically, as researcher did for old SEM machines.

2.1.1 Electron Column

The most important portion is electron column. It is consisted on electron gun, electron beam, condenser lenses, spray aperture, deflection coils, specimen chamber, X-ray detector, vacuum and secondary electron detector. The main focus is emphasized at the small diameter. Thermionic emission is necessary for the generation of electron beams. These beams are produced with tungsten filament at suitable temperature, under vacuum in electron gun. Electrons are accelerated towards the anode that adjusted from 200 to 30 KV. Filament inside it controls the beams of electrons.

In the next portion the electron beam passes through the anode influenced by two condenser lenses, converge them into a focal point as shown in Figure 2-1. The accelerating voltage and condenser lenses are primarily responsible for determining of the

intensity of electron beam, when it will strike the specimen [45]. Electron column with labeled is shown in Figure 2-1.

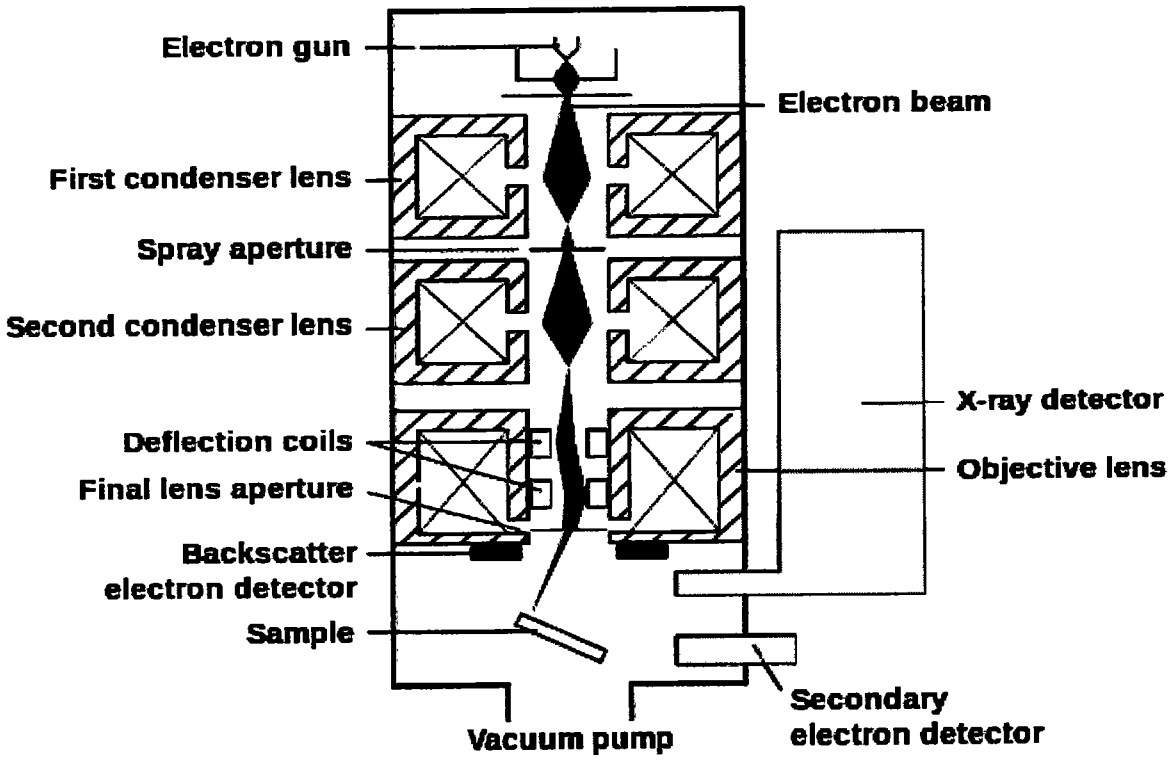

Figure 2-1: Scanning electron microscope column

Next to filament are aperture which are depends upon microscope. More than one aperture can also be used. The function of aperture is to reduce the extraneous electrons. Final lens at the bottom are used to determine the diameter as well as resolution. It also determines the value of depth of filed and its effect on brightness and resolution [46]. When beam of electrons reached the specimen, images are formed. A stigmator placed in objective lenses to control the aberrations of electron beam with the help of magnetic field. When the electron strikes the specimen it should have a circular cross section, but usually it was observed elliptical, that's why a stigmator is used to convert it into circular cross section [47]. The lower portion of column in which specimen placed is known as specimen chamber. The secondary electrons from specimen attracted towards the detector by positive charge.

2.1.2 Vacuum System

A vacuum of approximately $5x10^{-5}$ Torr is required to control the beams of electrons in electronic column. The vacuum in column is also required due to main three reasons.

- Column optics can work freely in a dust free atmospheric pressure.
- Dust particle and air present in the column can interfere and block the electrons to reach the specimen.
- The current passes through filament causes it to reach the amount of 2700K.

So for adequate pressure two or more than two vacuum pumps are present in electron vacuum portion, for example turbo molecular pump, mechanical pump etc. Moreover pressure less than 10^{-2} Torr is very easily to obtain with the help of turbo molecular pump. This pump can rotate at 20,000 to 50,000 rpm to pumped out all gasses as well as air to made a vacuum in the vacuum column [48]. SEM machine name FEI Quanta is designed to perform with low and high vacuum [49, 50].

2.1.3 Electron Beam Specimen interaction

Originally microscopy can be obtained with the help of light microscope, specimen resolution of the order of 0.2 microns. Electrons beams can be used as illuminated source instead of light, which allows resolution of 25 A°. The beam of electrons can give a better resolution, as well as provide variety of signals that are useful for the information related to cauterization of the surface of the sample.

The electron beam interact with the specimen which yield back scattered electron as well as secondary electrons, they receive in the form of signals continuously, as long as the electron beam interact with specimen. Microscopic inspection of specimen produces different signals because of two separate type of interaction. Secondary electrons are produced due to collision of scattered and of incident electrons (inelastic collision). Back scattered electrons are produced due to collision between scattering electron and specimen electron or with nuclei (elastic collision).

Instead of this many signals are produced in scanning electron microscopy. One of them is X-ray signal that produced due to the recombination process of the electron and positron within the specimen material. These X-rays are important for determination of elemental composition through EDS (Energy dispersive x- ray spectroscopy) analysis for characterization of x ray signals. Figure 2-2 represents the possible interaction and its results in the form of X-rays, secondary and back scattered electrons.

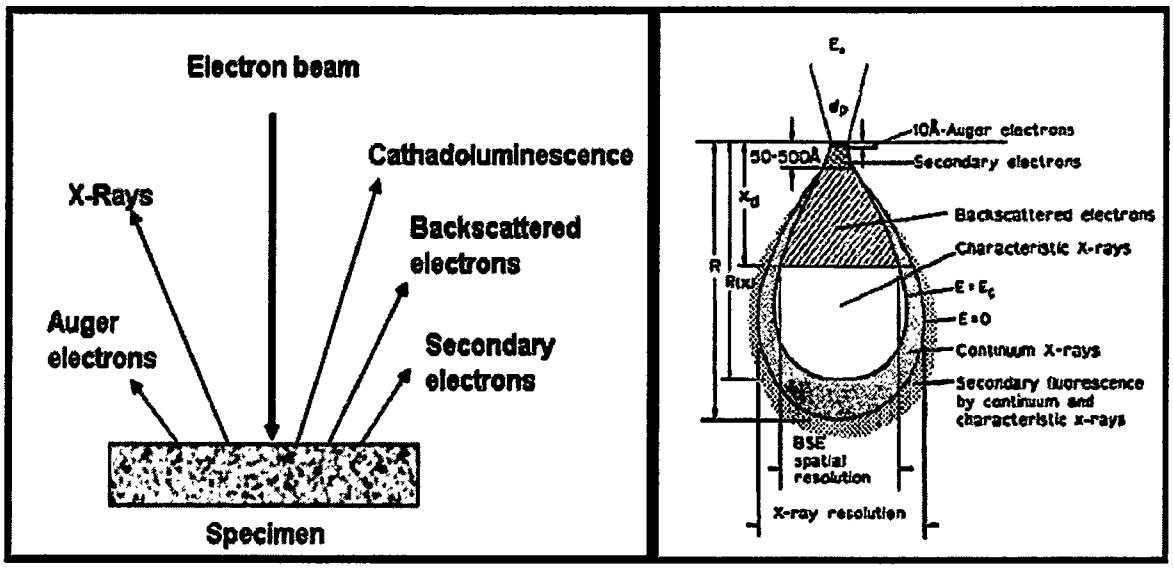

Figure 2-2: Signals that shows results from electron beam specimen interaction.

2.1.4 Observation Techniques

With the advancement in new technologies made it quite easy to observe and analyze SEM image. A short training is required to obtain a good image. For a new or immature user it seems difficult to obtain satisfactory, sensitive and broad wide image in complex scenario with good resolution.

2.1.5 Image Disturbance

Image disturbance caused during imaging the sample by SEM machine. There are two types of error usually observed. The first disturbance due to the defects in instrument and secondly the more likely disturbance caused by human error. Improper sample preparation is one of the most important errors for image disturbance. Additionally, external influences may damage the image or disturb it. Vibrations are also important factors for an image disturbance. Figure 2-3: Shows the images disturbances in SEMs.

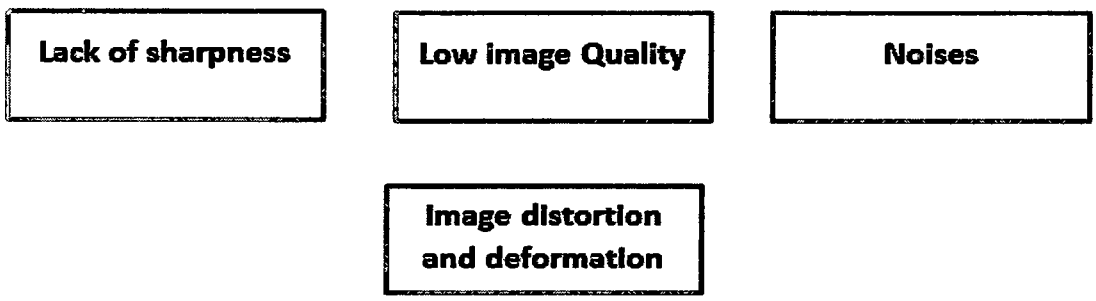

Figure 2-3: Images disturbances in SEMs

2.1.6 Effect of accelerating voltage

The major issue is a clear image. Accelerating voltage has a large influenced at on image. The voltage depends upon the specimen being examined. The most conductive material can behave better at high voltages. Perhaps higher voltages (15 to 30 kV) are required for high magnification and large resolution. If the material is not highly conductive, higher voltages can damaged the material. So for polymers and ceramics less than 10 kV is suitable value for imaging them. For high accelerating voltage one can obtain a high resolution but deficiencies are broad while imaging the specimen such as unclear surfaces structures, the more edge effect, more charge up and more damaged. Contrary at low accelerating voltage we obtain low resolution with clear surface structure, less damaged, less charge up and less edge effect.

2.1.7 Effect of working distance

A good quality image is always a keen interest of a researcher, besides the accelerating voltage work distance is also have greater influenced at the image. For good result generally 10 mm distance has been used for good depth field while maintaining high resolution. At low accelerating voltage and reduced work distance below 10 mm, one can obtain a good resolution. So small work distance can produced a high resolution with smaller depth of field, while for a large working distance we can obtain a large depth field with low resolution.

2.1.8 Effect of spot size

Another important effect is spot size, which basically restricts the beam current. The beam current restriction caused the contrast compensation and brightness. If the aperture size is large, it will produce large current with low resolution and smaller depth of field. On the other hand if aperture size is small, this results in high resolution with greater depth of field and grainy image.

2.2 X- ray Diffraction

XRD is a rapid analytical technique consist on dual wave particle nature, used for primarily purposes such as phase identification and characterization of a compound based on their diffraction pattern. It can provide information up to a unit cell dimensions and become a common technique for crystal structure and atomic spacing. X-ray passing through a crystalline material produced pattern used to identify the pattern of the unit cell.

X-ray passing to a crystal bent it into various angles, the process is known as diffraction and it interacts with electron in material for an electron cloud [51]. The angle depends upon the diffraction of x rays between the adjacent layers of the atoms of the material. For adjacent angle the X ray absorbs the energies when they are in phase.

2.2.1 X-ray generation and properties

X rays are known as electromagnetic radiation. The photons energies for X-ray lie in between of ~ 100 eV to 100KeV. For diffraction, until now only hard X-rays of short wavelengths ranged 1keV to 120 k eV. Wavelengths of x rays are comparable to that of an atom, so they are ideally suitable for structure arrangements of atoms or molecules in an atom. For bulk structures these hard X-rays penetrate deep and provide the structure of the material. Usually x rays are produced by either X-ray tube, but with tremendous progress in this field one can obtain x rays with synchrotron radiations.

X-rays are generated when an electron beam accelerated across a high voltage field bombarded at a stationary or moving target. Then electron collides with atoms and slows down. As a result, continuous spectrum of x rays emitted, known as bremsstrahlung radiations. The high energy electron also ionized and emits the inner shell electron of the atom. When an electron fills the shell a photon with X-ray characteristic energy emitted. Common targets used in X-rays tube are Mo and Cu. Cu emits 8 keV of x ray with 1.54 A° and contrary Mo emits 14 keV of x ray with 0.8 A°. In recent years Synchrotron facilities becomes the major source which enables to measure the x ray diffraction. These sources are thousand to millions times more intense in comparison with laboratory x ray tubes.

2.2.2 Lattice plane and Bragg's law

The electrons primarily interact with the atoms and molecules, some of the interacted X-rays are bounced back with the same path. In the interaction of X-ray with electron, if there is no loss of energy in X-ray photon (Reflected) then the interaction is totally elastic. In this process only momentum transferred between X-rays and electron. This scattering also named as Thomson Scattering. These X-rays are measure in diffraction experiments that carries information about the electron distribution in the material. Contrary when electron interacted with X-rays some of the energy will be transferred between them, then this type of scattering is known as inelastic or Compton scattering.

Diffracted waves can interfere with each other, which results in strong modulation of intensity distribution. If atoms are arranged in periodic pattern as we found in crystal, the diffracted waves will consist of sharp interface called maxima with the symmetry of an atom. Hence measuring of the diffracting pattern can give us the distribution of atoms in material.

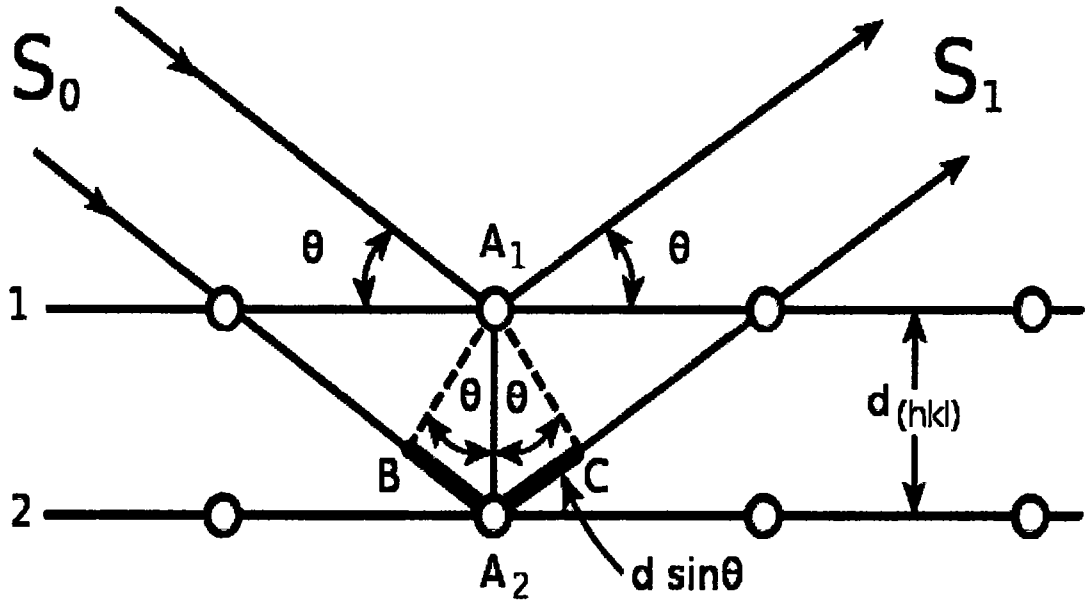

Figure 2-4: Lattice distance and Bragg's Law

The peaks in X- ray diffractions are directly related to atomic distances (d). For Figure 2-4 the X- rays interacts with the atoms shown as 2-D in and periodic pattern. The condition can simply related as

$$n\lambda = 2d\,sin\theta \quad \text{---------- (1)}$$

This is known as Bragg's law and he was the first who proposed this theory [50]. In the above equation λ is the walength, d is the interplaner distances and θ is the angle between reflected and incident ray. This law is the most important one to measure the data of diffraction.

2.2.3 Powder diffraction

The most widely used technique is powder diffraction for characterizing of material. In Powder diffraction the sample consist of powder. Powder has tiny grains of crystalline material to be characterized. The technique is also useful for polycrystalline solid bulk and studying particle in suspension. In powder diffraction the crystalline domain are

randomly oriented in the sample, in 2D powder diffraction shows concentric rings of scattering peaks corresponds to various d spacing in the crystal lattice The peaks and it positions are helpful for identifying the structure of the specimen or material. For example the phase difference in graphite and diamond are different perhaps the both material consist of carbon atoms. Figure: 2-9 shows the liquid phase sample at right side and transmission mode sample at left side.

2.2.4 Thin Film diffraction

This is not a specific technique; instead it is a collection of many XRD techniques. These techniques are used to characterize thin film. These thin film samples are grown on substrates.It is an important process because hard X-ray can penetrate through the epitaxial layers. Some special precautions that are necessary to be made; first substrate is too thick for transmission, so all we need is reflection geometry. Secondly, high angular resolution is required. The sharpness is due to very low defect densities in the material. Basic XRD measurements made on thin film samples consist upon precise lattice constants, rocking curve, super lattice, glancing incidence x-ray reflectivity and texture.

2.2.5 Texture Measurement

It is used for uniform distribution of the particles or grains in the material. Material can be termed as texture if and only, the particle are aligned in the orientation along certain lattice plane. With the help of texture one can analyze the difference between polycrystalline powder and single crystal. It is used in fabrication process of thin sheet metal.

Texture measurement can also be referred as pole figure. It is plotted in polar coordinates. The pole graph figure data as displayed as counter plots or elevation graph with zero angle in center.

2.2.6 Small angle X-ray scattering

Small angle X-ray scattering referred as SAXS, are concerned with angle $< 1^{\circ}$. According to Bragg's Law, the diffraction information about structures with large d-spacing lies in the region, so the Small angle x ray scattering technique is commonly used for probing large length scale structures, i.e., high molecular weight polymers, self-assembled superstructures and biological macro molecules. There is small angular separation in

direct beam and the scattered beam, this lead to the challenging state for small angle X-ray scattering measurements.

2.2.7 X-ray Crystallography

The standardized technique is X-ray crystallography used for identifying crystal structures. The basic theory was presented after the discovery of X-rays. However it took much time for development and instrumentation. With the advent of synchrotron radiation sources and modern computer technologies enable the X-ray crystallography.

Phase identification of is the major problem in X-ray crystallography. The data does not depend upon phase of the structure as it depends upon amplitude only.Since the last couple of decades many newly developed methods has been introduced for identification of phases. Among them computationally based direct method, isomorphous replacement, and MAD method are famous 51].

3. Experimental Work

In this chapter, details are given of experimental setups; experimental procedures relating to the methodology adopted to obtain the results are discussed. Experimental work depends upon the graphene production via modified Hummer's method. Its Raman analysis and microscopic analysis are mentioned in detail. Further in powder metallurgy, process of mixing of the materials in Ball milling, compacting of material and sintering of green compacts are also expressed. The hardness and density measurements of material are also performed. Preparation of samples for microscopy is mentioned in detailed. On the basis of all characterizations techniques mechanical properties are discussed in next chapter.

3.1 Materials

Graphite flakes powder, 23% concentrated H_2SO_4, NaNO3, 30% pure H_2O_2, $KMnO_4$ received from PINSTECH (Material division) Pakistan. All the materials are used same, as they were, without further purification.

Aluminum has broad family of alloys, but the most useful alloy, 6061-Al was used with a particle size range of 20-60 μm, B_4C powder with mean particle size range of 50 μm and Graphene with particle size 30 μm were used as starting materials. Table 3-1: gives the composition of 6061-Al alloy.

Table 3-1: Composition of 6061-Al alloy powder (given in mass percentage)

Alloy	Cu	Mg	Si	Cr	Fe	Zn	Al
6061-Al	0.31	1.02	0.53	0.1	0.062	0.007	Bal.

3.2 Production of Graphene

For the production of graphene there are two methods. First preparation of graphene by modified Hummer's method and, second by breaking graphite with ceramic matrix powder using high energy ball milling. However graphene was carried out by modified Hummer's method (solution Method), which is top down approach.

Initially commercially available, 1 gram of graphite powder with 0.5 gram of $NaNO_3$ and 23 ml of H_2SO_4 are mixed up under constant stirring for 1 hour at room temperature. After mixing of powders, added 3 gram $KmNO_4$ gradually under constant stirring while keeping whole solution in an ice bath so that, the temperature could be maintained

below than 20°C to avoid explosion. Once $KmNO_4$ react with the above solution completely, stirred the solution at 35°C for 18 hours. Next added 500 ml of de ionized water and kept it for 1 hour, further treated itdrop by drop with 15 ml of H_2O_2. After the reaction of H_2O_2, the solution was divided into two parts , with the passage of time graphene oxide layers were at the bottom of the flask, by filtering it, we obtained graphene oxide (GO).

Graphene oxide was treated with 15 ml HCL and 5 ml H_2O_2 and heat up for 4 hours at 98°C temperature. After four hours graphene oxide was converted into reduce graphene oxide. For removal of impurities from graphene, repeated the steps for three times by heating the material with constant quantity 15 ml HCL and 5 ml H_2O_2, we obtained reduced graphene oxide, which is commonly known as graphene.

3.3 Ball Milling

Mixing was performed in a ball milling grinder for powder metallurgy developed by RETSCH (Germany). The volume of B_4C and 6061-Al was fixed 4.0 % and 96 %. To check the effect of graphene via comparison the volume of B_4C, graphene and 6061-Al was fixed 4.0 %, 1.5 %, 94.5 % respectively. First B_4C with 4 % with 6061-Al was grinned in bar mill jar. Next all three powders (6061-Al, B4C and graphene) were kept in ball milling jar. Two tungsten balls, each weighing 5g, were added in jar mill such that the ball to powder ratio was 1:10 in both powder milling.

Table 3-2: Experimental parameters used in ball milling

Mixing Type	Wet milling	Wet milling
Composition by weight	96% 6061-Al alloy + 4.0% B4C	94.5% 6061-Al alloy + 4.0% B4C+1.5% graphene
Revelation of Ball mill per second	300 rpm	300 rpm
Gas used	Argon	Argon
Liquid Pendulum	Toluene (1 ml per g of powder)	Toluene (1 ml per g of powder)
Ball ratio	10:1	10:1
Time period	2 hours, 3 hours, 4 hours	2 hours, 3 hours, 4 hours

For mixing the Jar was covered with special lid so that no air can entered in ball milling jar. The lid has the provision to purge gas inside the ball milling jar. Wet mixing was performed; toluene was added to the powder in the ratio of 1 ml per gram of powder. Ball mill was performed at a revolution speed of 300 rpm for 2 hours, 3 hours and 4 hours respectively. So, a total of 6 experiments were performed in this study. (No variations in mixing environment coupled with six variations in mixing time)

Table 3-2: summarized the mixing parameters of graphene, B_4C and 6061-Al in ball milling.

3.4 Drying and Compaction

Once the process of ball milling of material was completed, Tungsten jar was removed from the mill. Further step in PM is drying and compacting. Before compacting the 6061-Al/B_4C and 6061-Al/B_4C/graphene powder was heated up to 130 °C in an oven to remove the toluene in the powder for 3 hours, whereas the boiling point of the toluene is 110.6°C. Drying for 3 h at a temperature higher than boiling point of toluene ensured its complete removal from the mixed fine powder.

Cold compaction was done using LBM, type MB 20, hydraulic polluting press. 5 g of powder was filled in a die having diameter 19 mm. Static acid was used as the die lubricant. 500 MPa load was applied to form a solid cylindrical pellet. Three pellets from each batch were prepared. After the green compacts were formed, green density of the pellets was calculated.

3.5 Pressure less Sintering

After drying and compaction the next stage in powder metallurgy was pressure less sintering. The pressure less sintering is commonly used for hybrid composite, which requires a relatively long time, high temperature for processing. These two parameters provide grain growth and simultaneous degradation of nano fillers. Pressure less sintering was carried out in a tube furnace, type RSR3 developed by Ruhstrat (Germany). The sample was marked according to milling time. They were kept in the furnace tube. Temperature was increased with an interval of 5°C and then maintained a 400°C for two hours in the absence of pressure. Latter it was increased in an interval of temperature 5°C to achieve 630°C and kept it for 1 hour. The green sintered compacts called pellets were allow cooling at room temperature in air for a specific time. Whole phenomenon is expressed in Figure 3-1.

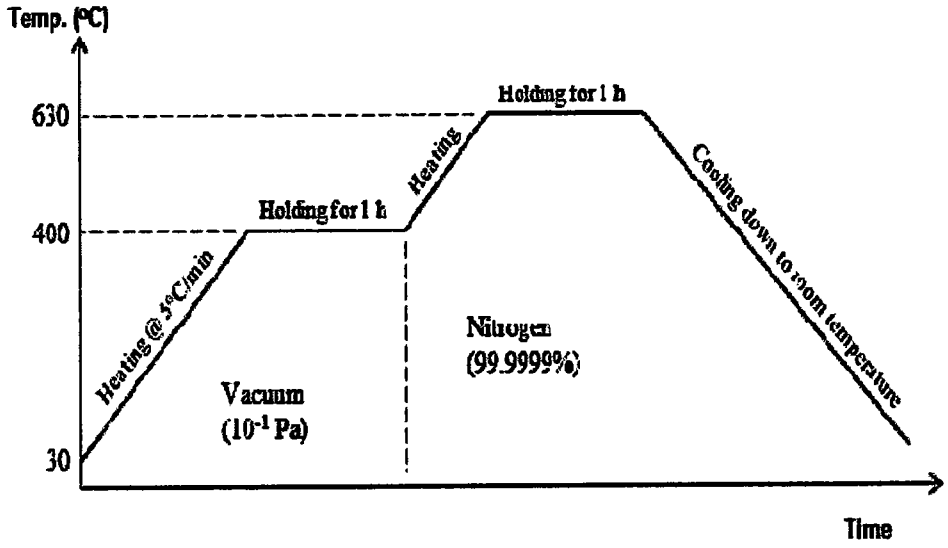

Figure 3-1: A complete cycle for Sintering time mechanism

3.6 Density & Hardness Measurement

Sintering consolidatethe materials and made them hard to acquire a bulk solid shape. The density of the samples was determined using Archimedes principle. In this method, weight of the sample in dry air and that in water were noted. Their difference equals the weight of water displaced by the pellet. Using this weight and density of water, volume of water displaced, or in other words, volume of sample was determined. Density was finally evaluated using this volume of pellet and its weight in air from the simple mass to volume ratio.

Hardness of the samples was determined using Karl Frank Rockwell Hardness Tester. Rockwell's B scale has been used in these measurements. Average of 3 readings has been reported in the results.

3.7 Microscopy

The sintered compacts after rolling were sectioned from the longitudinal cross section for metallographic studies. The samples were grinded and polished on automatic polishing machine (Struers TegraForce-5) by optimizing the metallographic procedure to obtain scratch free microstructure.

The polished surface of Al/B_4C and Al/B_4C/graphene was examined under Scanning electron microscopy (SEM), and XRD analysis.

4. Results and Discussion for Graphene

In this chapter details are given for the results of graphene synthesized from modified Hummer's method. The characterization techniques that were undertaken are Raman spectroscopy analysis, Scanning electron microscopy (SEM), and X-Ray diffraction (XRD) patterns.

4.1 Raman Analysis

Despite the wide use of the graphene, the identification of graphene and counting of layers is not an easy task. The advantage of graphene is the possible advent of planar technology, which is compatible with fabrication process [52]. During exfoliation of graphene it may damage the structure; therefor it is good to analyze it by some appropriate way. So a well-known approach, known as Raman spectroscopy is a perfect selection for characterization, as it is non-destructive, fast and has a high resolution. It can provide maximum structural and electronic information. Consequently Raman spectroscopy becomes standard for fast growing field of graphene. The spectra obtained from Raman spectroscopy is very simple, just a couple of band between 1000 cm^{-1} to 2000 cm^{-1} region. Their shapes, position and intensity allow us to differentiate between amorphous carbon and metallic nano tubes [53]. Raman spectroscopy can deal with one or multilayer, but when the layers exceed more than 5 layers, it would be difficult to analyze data with Raman spectroscopy.

Graphene the most important reinforcement has been characterized with XRD and SEM patterns. Reduction of graphene from graphite can be study by using Raman spectroscopy. The main features are D and G peaks in graphene. G stands for graphene peak and the D stand for disorder peak. Furthermore the D band also shows the defectiveness in the material. Using the ratio of peak intensities of D and G, one can use Raman spectra to characterize the level of disorder in graphite and its derivatives.

Pure graphite only shows a G band. This band is due to the stretching of the sp^2 bonds, while graphene oxide and graphene have a G band as well as D band. The increase in I_D/I_G ratio is due to the decrease in average size of the sp^2 domain upon reduction. The G peak is due to the doubly degenerate zone center E_{2g} mode [54, 55]. As zone-boundary phonons do not satisfy the Raman fundamental selection rule. So such phonons give rise

to a peak at 1350 cm^{-1} in defected graphite, called D peak. [56] These peaks are dependent on laser excitation energy [57].

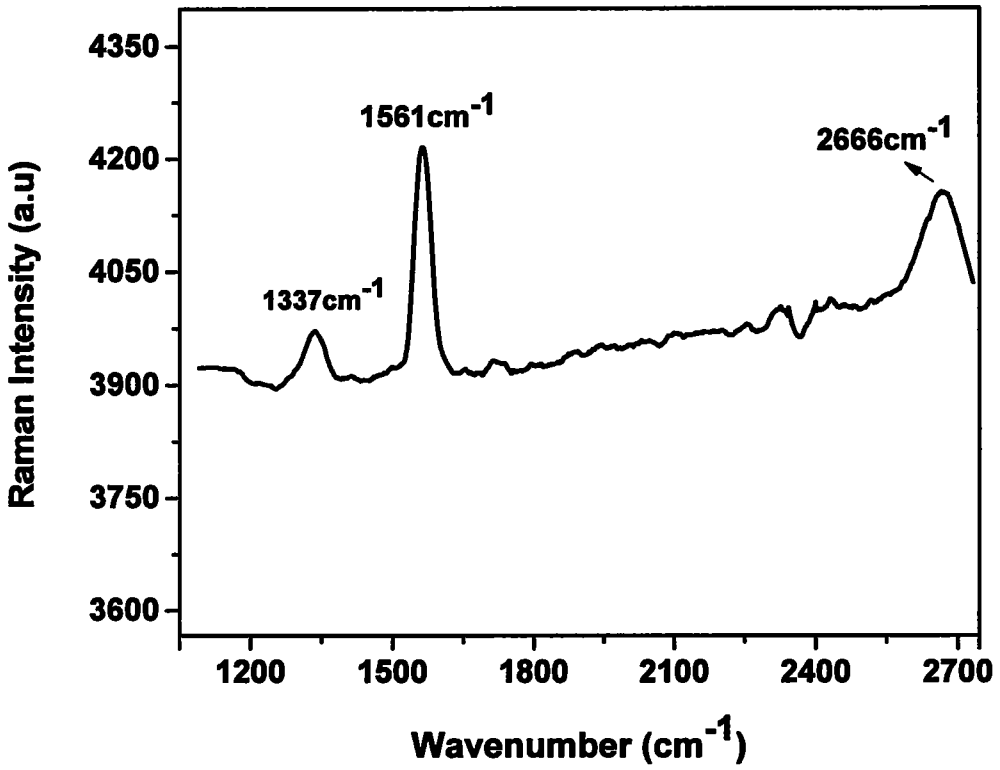

Figure 4-1: (a) Raman spectroscopy of Graphite

The Raman spectra of graphene, graphene oxide and graphite were measured with 550 nm excitation of He-Ne laser. In literature the G and D peaks for graphite are 1582 cm^{-1} and 1350 cm^{-1} respectively [54-56]. In figure: 4.1(a) shows the most intense feature D and G bands have slightly shifted to left with short wavelength. The value was observed for D and G band at 1337 cm^{-1} and 1561 cm^{-1} respectively. The 2D band was also observed at 2666 cm^{-1}. These values are closely related to the values given in the literature. While I_D/I_G value is 0.9244 for graphite.

Figure: 4-2 shows the Raman analysis obtained for graphene oxide showing D and G bands at 1356 cm^{-1} and 1605 cm^{-1}, respectively. While a D′ band was also observed at 1720 cm^{-1} and 2D at 2689 cm^{-1}, which are almost similar to the data presented for graphite in Fig: 4-1. While I_D/I_G value is 0.9974 for graphite oxide. It was also observed that, the peaks are slightly shifted right with long wavelength, and intensity of G band also reduced in comparison with graphite Raman spectra.

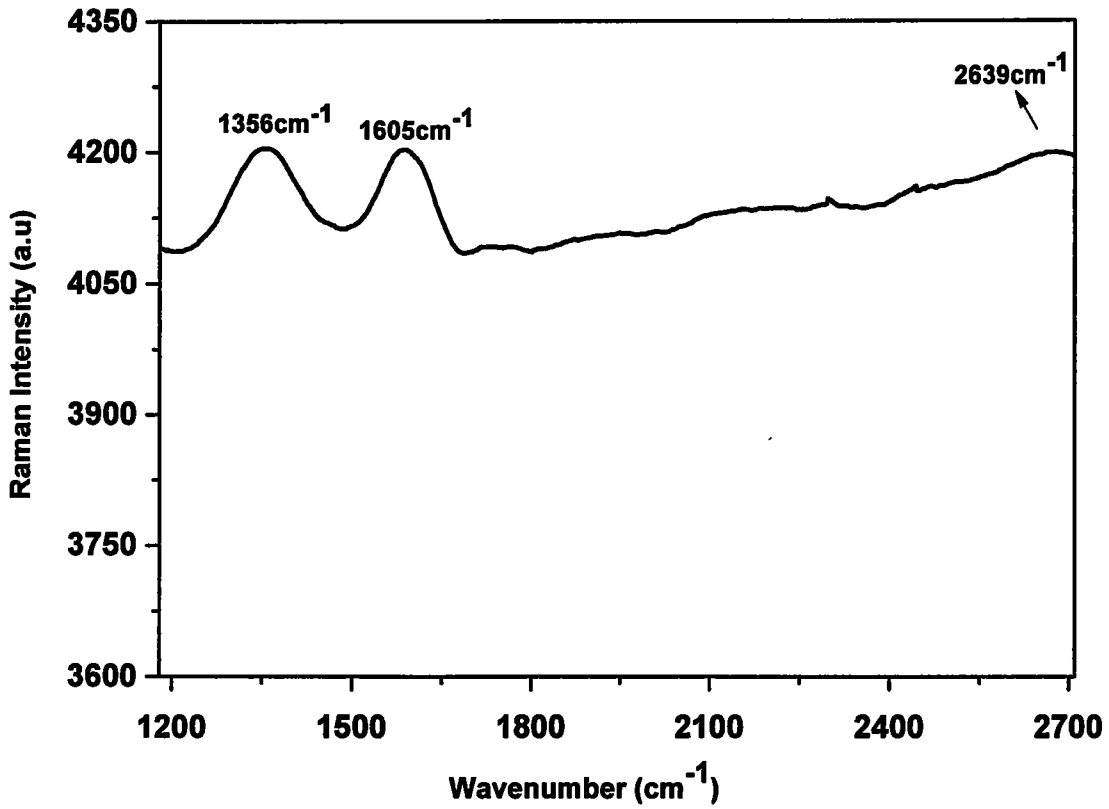

Figure 4-1: (b) Raman spectroscopy of Graphene oxide

In literature of Raman spectra of graphene, stokes phonon energy shifted by laser excitation and produce three main peaks, first G at 1580 cm^{-1} and second 2D at 2690 cm^{-1} while third D peak at 1350 cm^{-1}.

In comparison with literature value we have observed D and G peak at 1358 cm^{-1} and 1593 cm^{-1}, respectively. The I_D/I_G for graphene is 0.9937, which displays two different behaviors. At low defect density I_D/I_G will increase, while at higher defect density creates more elastic scattering. The value of I_D/I_G gives us multilayers for graphene in sample, which shows that the value decreased significantly due to increasing defect density result is in a more crystalline carbon structure in graphene.

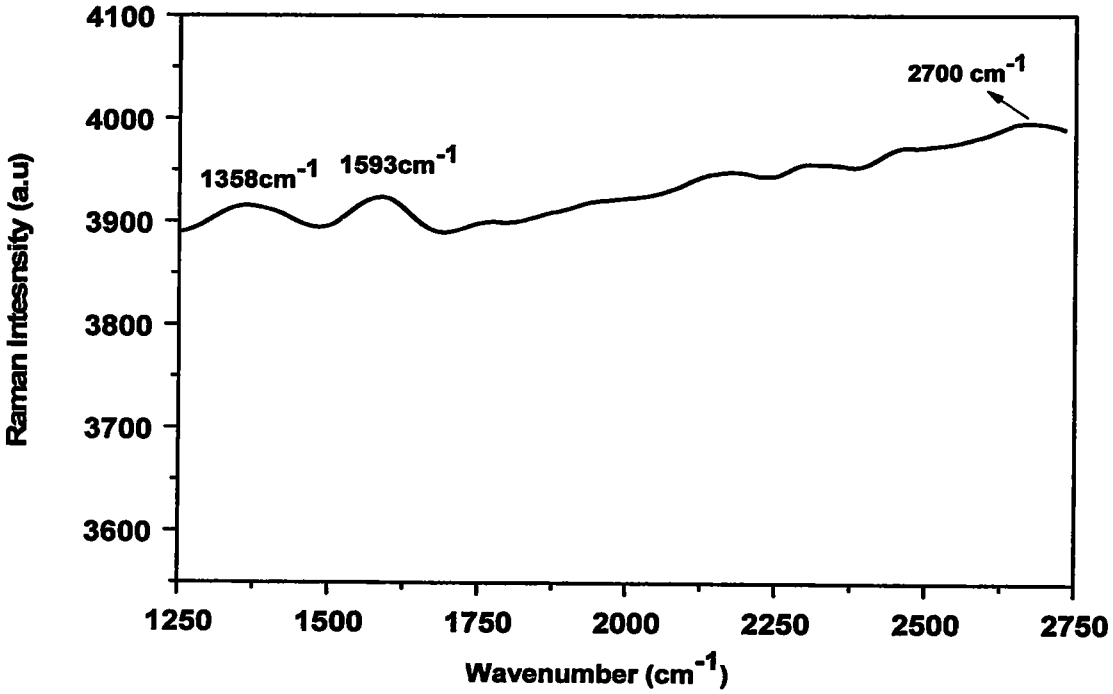

Figure 4-1: (c) Raman spectroscopy of Graphene

In comparison of Figures 4-1 (a) (b) (c), it shows that the D and G peaks have slightly shifted to right side in graphite and graphene oxide, while in graphene; it was shifted to a little left. Contrary, at the other hand value of D band is greater in Raman spectra of graphene in comparison with that of graphene oxide and graphite. So Raman spectroscopy clearly identifies the D, 2D and G band in graphene, which is the true reason that the exfoliation of graphene with modified Hummer's method was done and few layers of graphene have been obtained.

Table 4-1: Summarized values of Graphite and its derivatives.

Band Type	Graphite		Graphene Oxide		Graphene	
	Literature data	Observed Data	Literature data	Observed Data	Literature data	Observed Data
D Band	1350	1337	1350	1356	1350	1358
G Band	1582	1561	1581	1605	1580	1593
D' Band	-	-	1625	1720	1620	1720
2D Band	2685	2666	2687	2689	2690	2700
I_D/I_G ratio	0.9244		0.9974		0.9937	

4.2 XRD analysis

XRD pattern for graphene synthesized by chemical reduction of exfoliated and intercalated graphene is presented in Figure 4-2. The XRD was taken with CuKa1 radiation (λ= 1.54A°). We have observed that, three strong peaks at 38.75, 44.75°, and 65.1°, corresponds to d spacing at 2.24, 2.10 and 1.47 respectively. They all related to 110, 210, 310 planes, respectively, which are labeled in figure 4-2.

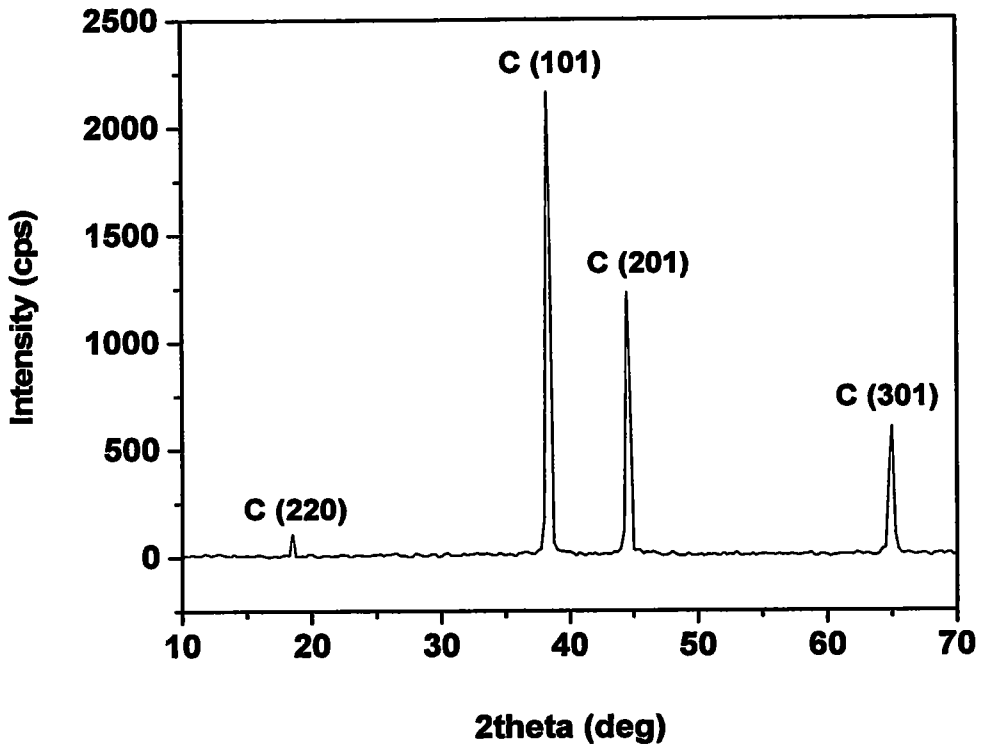

Figure 4-2: XRD Pattern for Graphene

The graph also reveals a very small peak with a small intensity corresponding to 220 plane of carbon with interlayer d spacing of 4.99 at 18.2°. It confirms the presence of the carbon presence in sample. The d spacing between the peaks provide a clearly indication that the structure of the graphene is crystalline and graphene has been reduced from graphene oxide via modified Hummer's method.

4.2 Microscopy

The morphology of graphene was observed with three SEM micrographs which are taken at 50 μm, 20 μm and 1 μm respectively.

Figure: 4-3 (c) at 50 μm shows clearly visible nano platelets of graphene. It is observed that the graphene nano platelets are irregular and folded. The layered structured of graphene nano platelets are observed, which are entangled with each other.

In Figure 4-3 (b) at 10 μm, it is evident that the same folded and irregular, entangled graphene nano platelets with large magnification. Similarly Figure: 4-3 (a) also clearly shows some entangled graphene layers. It was seen that the layers are stuck with each other providing sufficient information for graphene identification.

R. Perez-Bustamanate et al. have also observed few layers of graphene nano platelets by using modified hummer's method. They also stated that the graphene nano platelets were entangled and folded. Their results of Raman analysis of graphene are similar to those we have obtained for our samples [58]. The Raman analysis and XRD results have clearly indicated that the graphene has been synthesized.

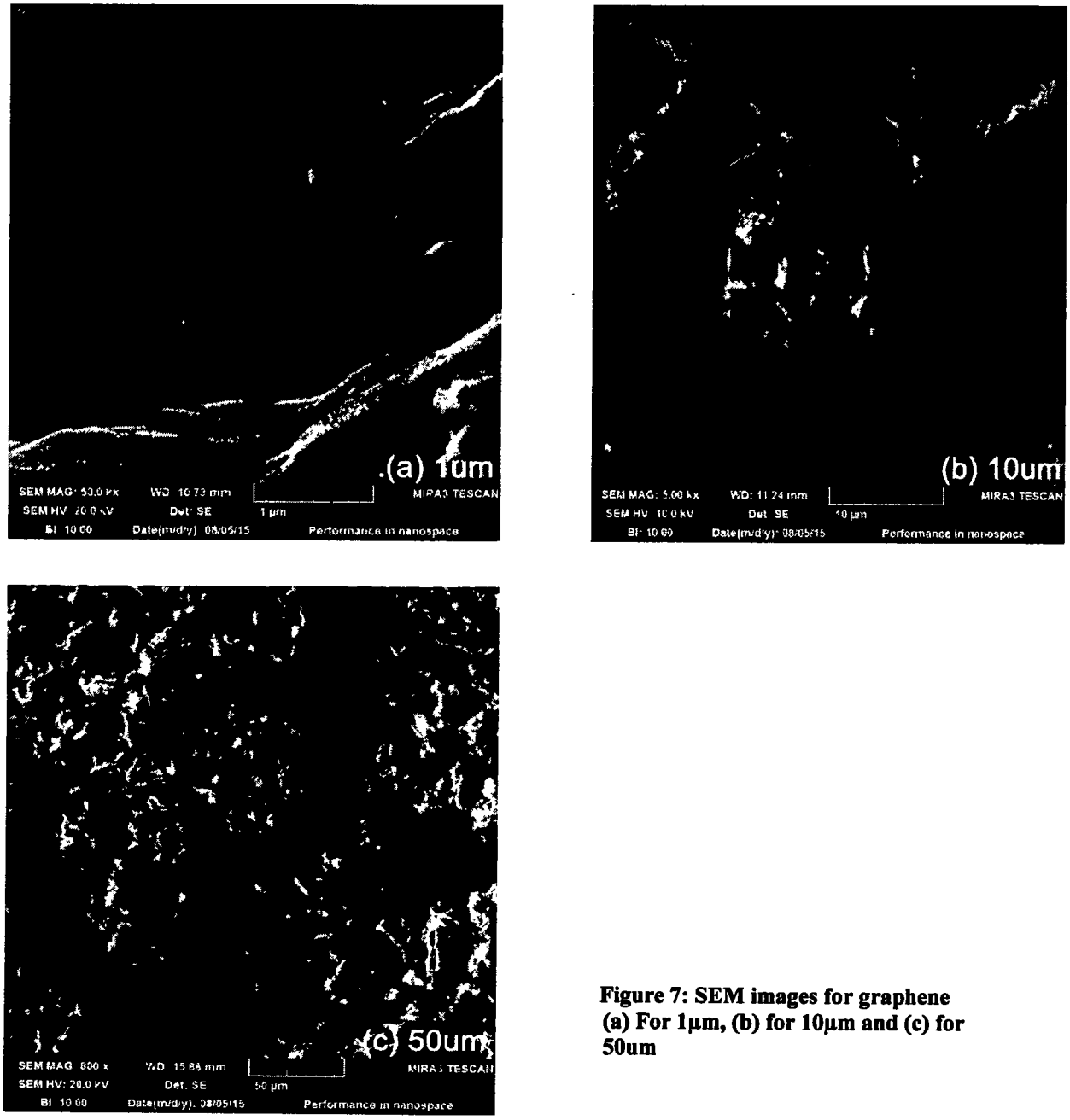

Figure 7: SEM images for graphene (a) For 1μm, (b) for 10μm and (c) for 50um

5. Results and Discussion for Composite

The experimental work majorly consisted of three main areas to be analyzed; the graphene synthesis, as discussed in previous chapter, secondly, effects of ball milling on morphology and particle distribution of 6061-Al/B_4C composites without additions of graphene have been investigated in detail, and thirdly effects of adding synthesized graphene nanoplatlets on the physical and mechanical properties of 6061-Al/B_4C composites also discussed in detail. Hardness measurements were undertaken to relate mechanical properties of 6061-Al/B_4C with 6061-Al/B_4C/graphene hybrid composites. Densities of the 6061-Al/B_4C/graphene composite were also measured to observe the effect of mixing time and sintering time on particle consolidation. In this chapter, the results have been presented in detail, followed by the discussion in the light of scientific facts.

5.1 Effect of Ball milling for Al-6061/B_4C

Figure 5-1 shows the ball milling effect of Al-6061/4.0 % B_4C at different time from 2 to 4 hours. For 2 hours ball milling, the B_4C particles break the aluminium particles as shown clearly in Figure: 5-1 (b, c). The size of particles was also reduced, but reduction of a large number of particles was not observed for 2 hours of milling. Figure 5.1 (a) shows the interaction of B_4C and aluminium at 2 hours, No definite change in alloy particles was observed at 2 hours.

For 3 hours of milling, aluminium particles change their shapes from spheroidal to long oval, which is clearly visible in Figure 5-1 (g). It was also observed that, the B_4C particles was also started to reduce in size and stuck with aluminium particles, hence to create a new surface with aluminium as shown in Figure 5-1 (e, f, g).

For 4 hours of wet milling all particles of aluminium alloy reduce in size. The reinforced particles break due to the pressure exerted by the balls in milling of powders. It was also observed that aluminium particles were reduced in smaller size in comparison with B_4C as shown in Figure 5-1 (h, I, j), B_4C is harder material than aluminium, so in interaction the surface of the aluminium break and changes as visible in Figure: 5-1 (I).

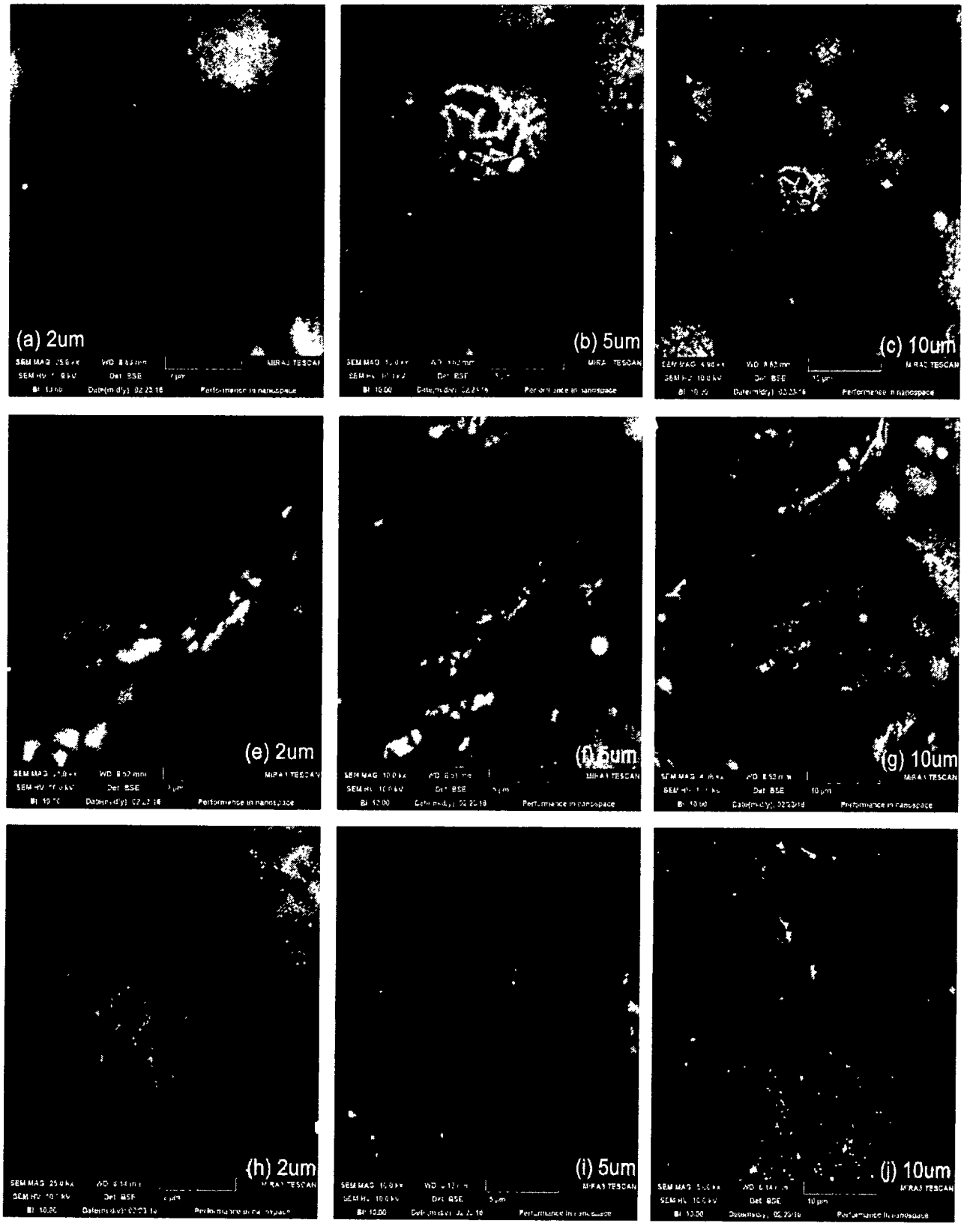

Figure 5-1: SEM micrographs for ball milled Al6061/B_4C (a, b, c) for 2 hours, (e, f, g) for 3 hours, and (h, I, J) for 4 hours.

The comparison of 2 hours, 3 hours and 4 hours ball milling reveals that, at 2 hours of milling has rendered the less reduction of particle size. For 3 hours of ball milling B_4C particles stuck with aluminium, hence sufficient to create new surface with aluminium. But uniform distribution and mixing was not good. For 4 hours of milling, the B_4C particles break as well as alloy particles, turned into smaller particle In short the particle size was smaller at 4 hours of milling, so a uniform distribution was obtained at 4 hours.

Study by Sharifi et al. (2011) on aluminum reinforced with boron carbide composites found that an increase in the milling time will resulted in uneven distribution of B_4C on the milling time of more than 5 hours compared to 15 minutes [59]. So for 4 hours uniform distribution has been achieved.

5.2 Effect of Ball milling for Al-6061/B_4C/Graphene

Figure 5-2 shows SEM images of effect of milling on the morphology of 6061-Al/B_4C/graphene milling at 2 hours, 3 hours and 4 hours, respectively. Aluminium particle size at 2 and 3 hours is greater than that of 4 hours of milling. This result is caused by milling effect of aluminium particle size. The particle size reduced in 4 hours of milling is caused by pressure exerted by the balls to powder during milling process. Therefore, particle breaks and become smaller in size at longer 4 hours of milling. For 2 hours of milling it was observed that the particle shape of aluminium powder was changed to a long circular rod, but only few of them were changed due to interaction of B_4C particles during ball milling with aluminium.

Figure 5.2 (a, b, c) shows the effect of 2 hours of milling, it is obvious that B_4C and graphene particles have scattered among the aluminum matrix. The increase in milling time caused the more uniform distribution of graphene and B_4C in aluminum matrix. For 3 hours of milling the B_4C and graphene particles were stuck with aluminum particles. The increase in milling time produced cracks in the particles, thus aluminum particles were broken down and form a new surface with graphene and B_4C particles.

Milling at 4 hours produced more even uniform distribution of B_4C particles, B_4C at 4 hours break down in to small pieces while the aluminium was also grinned to more small particles. The voids between B_4C and aluminum matrix was filled with graphene, thus produced more new surfaces between aluminium with B_4C and graphene. Hence in overall milling process the 4 hours of milling seems to be favorable, the uniform distribution were obtained as well as the particle size was much reduced.

Figure 8-2: SEM Micrographs for ball milled Al6061/B_4C/graphene (a, b, c) at 2 hours, (d, e, f) at 3 hours and (g, h, i) at 4 hours

5.3 XRD Analysis

Figure 5(a) shows phase identification analysis using X-ray diffraction (XRD) of Al/B_4C/Graphene composite milled at 2 hours. Two strong peak of aluminium were observed at angle (2θ ~ 38.5°) with plane 110 and (2θ ~42.17°) with 220 planes. A small peak with a very small intensity of Boron was observed at 23.25°. Some sharp peaks of B_4C with plane 313 and 002 observed at (2θ ~65.15°) and (2θ ~78.9), respectively. In addition a small peak of carbon at plane 002 was observedwhich was sandwiched between the peaks of B_4C. These peaks are the clearly identify that the reinforced graphene and B_4C make new surfaces with aluminum matrix, However a large amount of B_4C particle do not make part in plastic deformation as we have conducted sintering of composite in super solidus range.

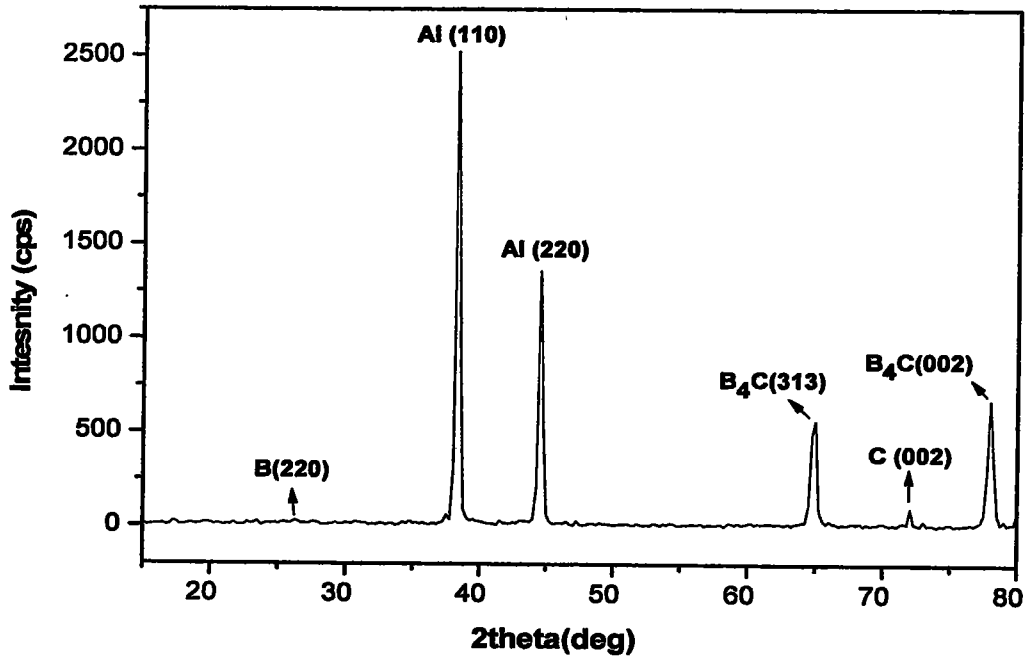

Figure 5-3: (a) XRD pattern for Al/B_4C/Graphene Composite at milling time of 2 hours

Similar effect were observed when the powder was milled for 3 hours shown in Figure 5-3 (b), In comparison with 2 hours milled powder we have obtained new narrow and small peaks of B_4C at an angle (2θ ~18.75°) with d spacing 4.394.

Figure 5-3 (c) shows quite a different pattern compared with other two. The strong peak of aluminium was observed at the same angle as mentioned above, but there were more than two strong peaks of B_4C were observed. A peak of carbon was also observed at (2θ ~41.5°).

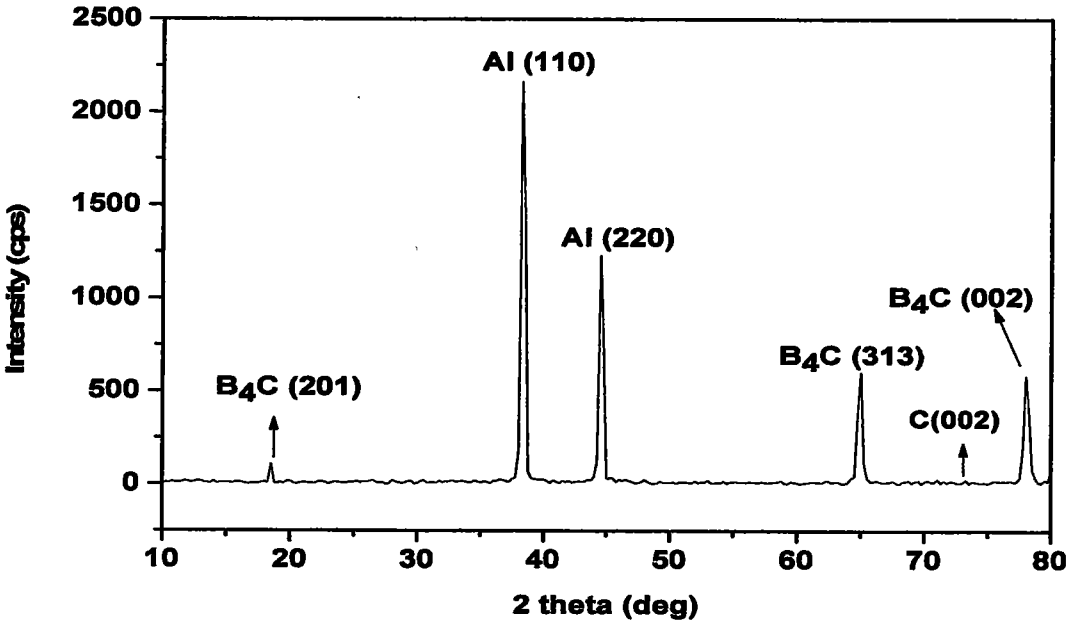

Figure 5-3: (b) XRD pattern for Al6061/B_4C/Graphene Composite at milling time of 3 hours

Figure 5-3 (c) also indicate that, as milling time was increased to 4 hours so the particle size has reduced as the result of an excellent plastic deformation was observed between aluminum and graphene, while B_4C particles do not take a part in deformation.

It was also observed that the crystalline of the material has increased with increase of milling time, which caused the grain size of the particle to decrease with an increase in milling time.

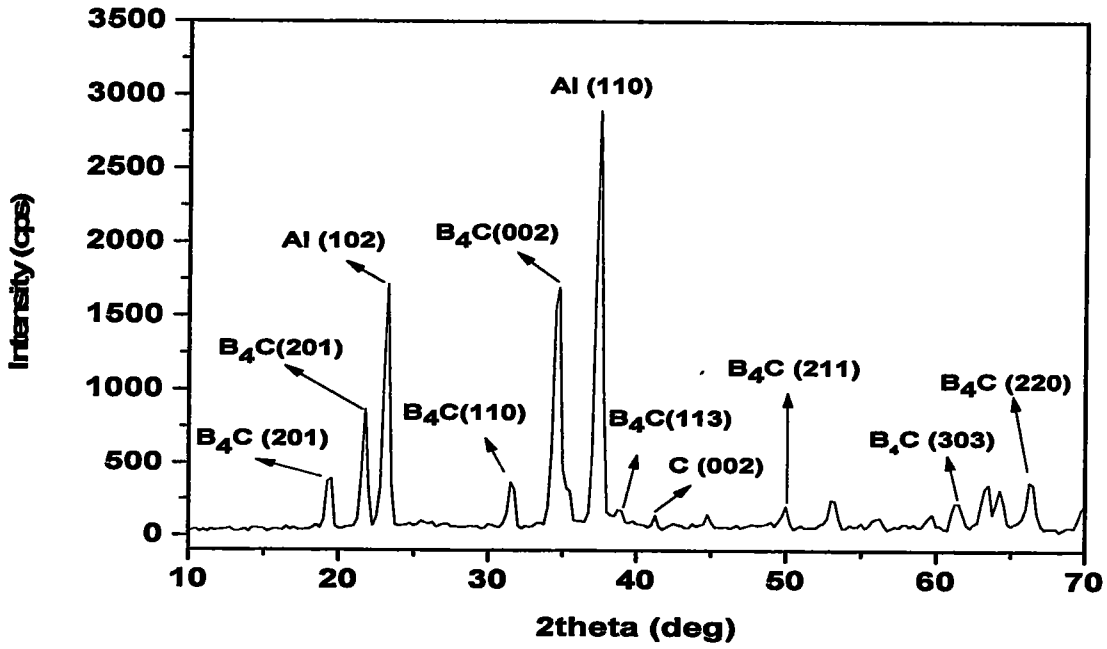

Figure 5-3: (c) XRD pattern for Al/B_4C/Graphene Composite at milling time of 4 hours

5.4 Morphology of Aluminium reinforced B_4C composites

SEM micrographs in Figure 5-4 show the evolution of morphology of composites at different milling times. In previous section" Effects of ball milling of 6061-Al/B_4C it is revealed, if we increase milling time, it will turn out in the form of more small particles. It was also stated that the uniform distribution was attained in 4 hours of milling but voids between particles was a major issue. So after sintering the pellets we have observed that the particle stick with each other and the voids diffuse during plastic deformation in pressure less sintering.

Figure 5-4 (a, b) which reveals the fact a uniform distribution was obtained after sintering the pellet. Some agglomeration of aluminium particles was also observed. Aluminium particle make only few new surface with aluminium particles, moreover instead of this at majority it just occupy the space in aluminium matrix and aluminium just stuck with B_4C. So at large scale formation of new surface was not observed in 2 hours of sintered composites, as shown in Figure 5-1(b).

A more even uniform distribution was observed at 3 hours in comparison with 2 hours of milling where B_4C particles was crack and stuck with matrix during milling and mixing. Following sintering the aluminium particles offers some plastic deformation but still, B_4C particle was fixed and do not make at large scale new surfaces with aluminium matrix. The reason behind the fact is that, B_4C required 2000°C to melt and we have used 630°C of temperature for sintering.

Figure 5-4 (e, f) shows a more even distribution during mixing and milling. The B_4C particles are broken into more small particles. After sintering the B_4C particles make new surfaces between aluminium and B_4C resulting in more even uniform distribution as shown Figure: 5-4 (e, f).

It was also observed, that in all sort of milling and mixing the porosities remains a big issue. The content of porosities for 2 hours was greater than of 3 hours and very low for 4 hours of milling. But with smaller size of particles, porosity was less at 4 hours of milling. Porosity leads to decrease in density, but it will deteriorate the hardness.

However the particles merged together in the matrix and the composite was well uniformly distributed in all six micrographs, and no agglomeration was seen at large scale in composites. Mohanty et al. (2008) in his study of fabrication technique and characterization

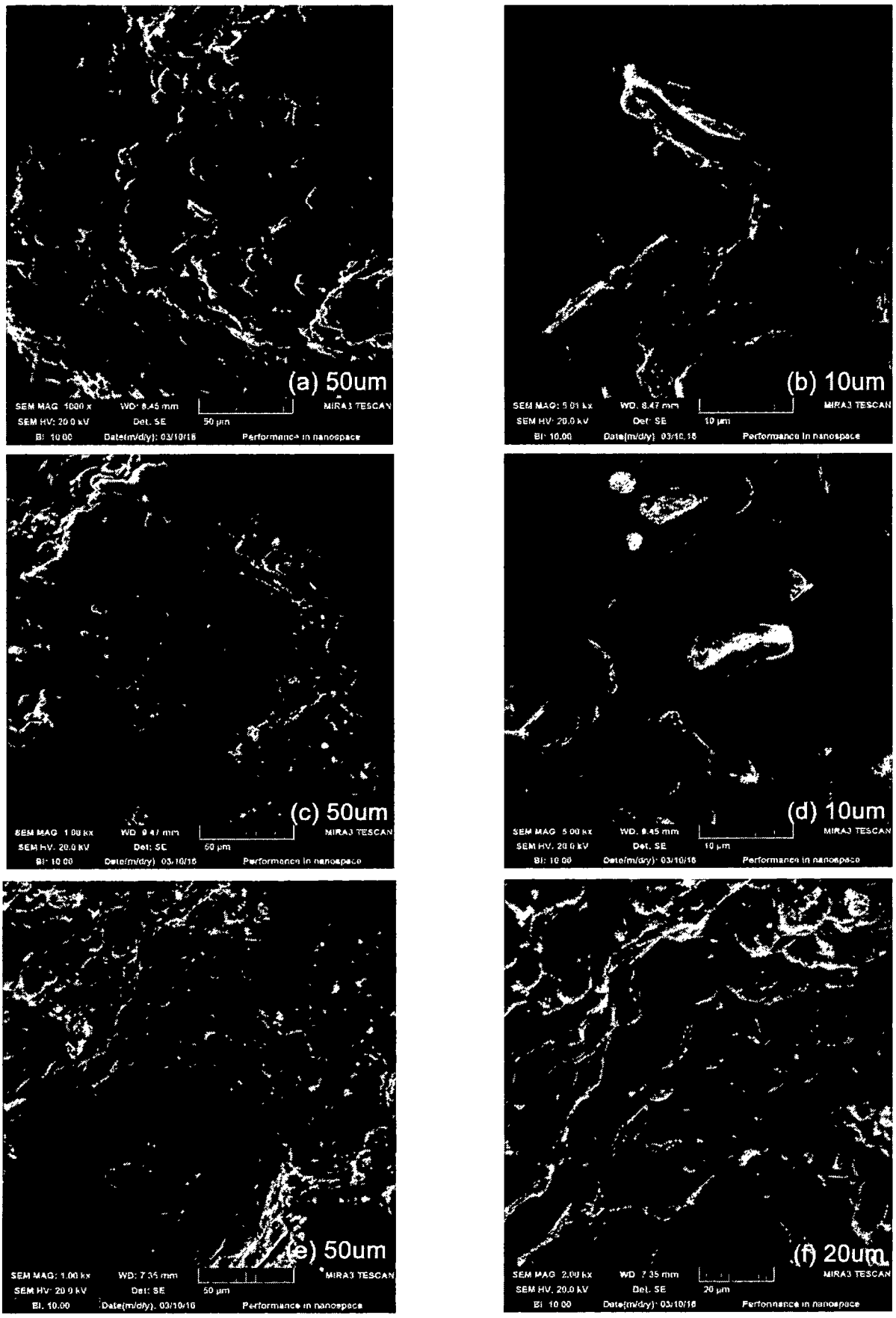

Figure 5-4: SEMs micrographs for Al-6061/B4C composites (a, b) for 2 hours, (c, d) for 3 hours, and (e, f) for 4 hours

of aluminium/boron carbide composites determined that an increased in Boron carbide content would decrease the density of the composite [27].

5.5 Effect of Graphene on Al-6061/B_4C composites

Effect of ball milling, with different variation in time, has been discussed in previous section. It was observed that aluminum particle was change their formation from spheroidal to long oval shape, it was also observed, at 4 hours of milling and mixing particles were uniformly distributed. With the comparison of 6061-Al/B_4C Sintered composites the 6061-Al/B_4C with graphene shows excellent results.

In 6061-Al/B_4C we have observed some porosity even at 4 hours of milling , where particles were uniformly distributed, but the scenario observe with the addition of 2nd reinforcement as graphene found changed. For 2 hours of milling the B_4C particles were not accurately grinned, but aluminium was cracked and turned into long oval shape which form new surface with graphene and B_4C as well. As a result, the porosity was less in the composite, which lead the density of the composite a slightly little higher as it was observed for hardness of composite as shown in Figure 5-5 (a, b).

For 3 hours of milled samples, the SEM shows also less porosity in comparison with 2 hours of sintered composite. Uniform distribution was also observed, Graphene plays a vital role as reinforcement.

For 4 hours milled sample, the minor porosity was observed, the graphene and B_4C make new surfaces at 4 hours sintered composites as the particles was uniformly distributed. The hardness of the 6061-Al/B_4C/graphene composite was increased in comparison with 6061-Al/B_4C composite.

So we can say that graphene play a vital role to achieve the primary objectives, which were; the lightest and hardest composite. These two primary objective were linked with uniform distribution of particle in the aluminium matrix, which were obtained with 4 hours of milling in which reinforced particles were grinned to small particles by exerting pressure with ball milling during powder metallurgy.

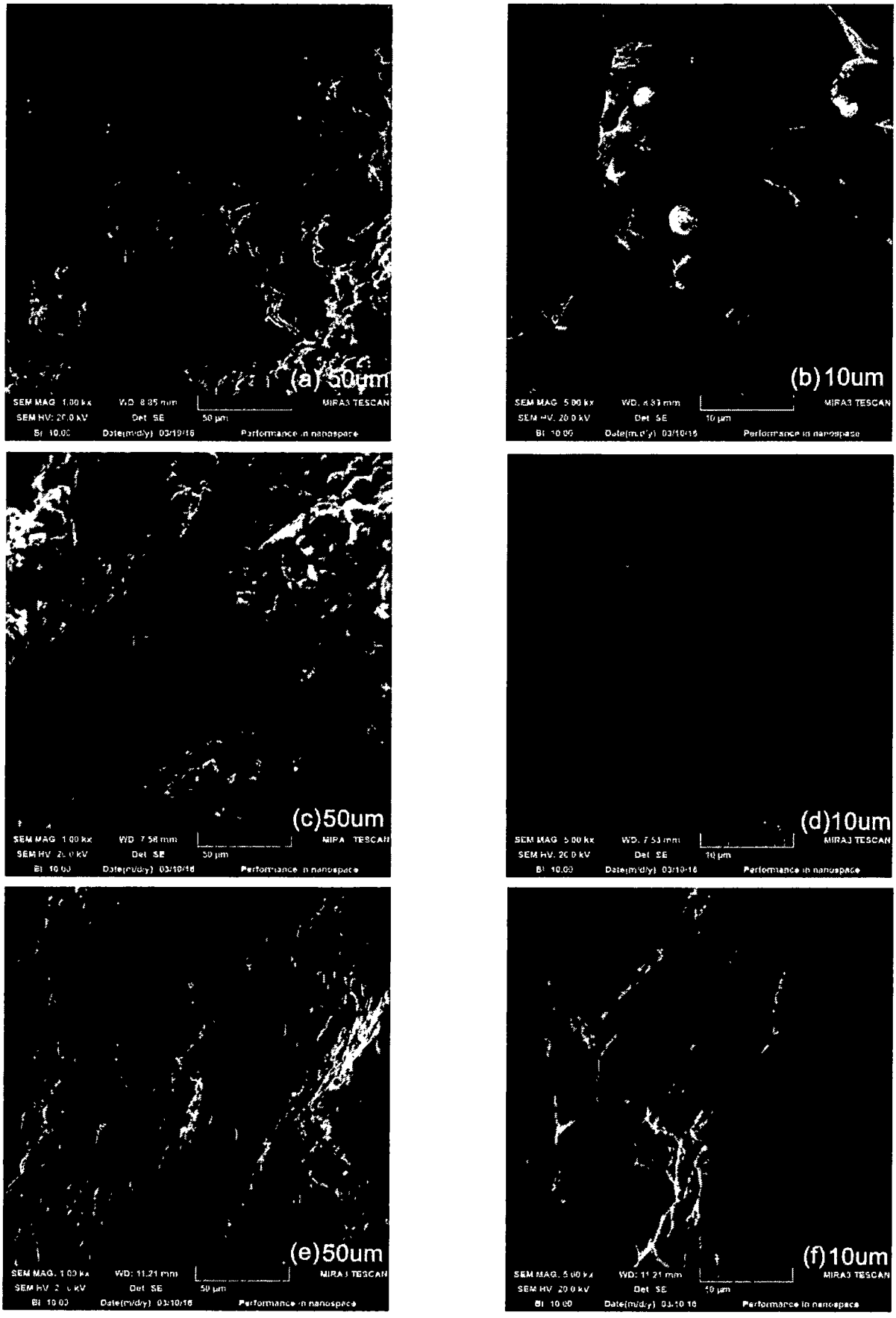

Figure 5-5: SEMs for sintered composites of Al6061/B_4C/graphene (a, b) for 2hrs, (c, d) for 3hrs, and (e, f) for 4 hrs.

5.4 Density

Immersion density values of Al/B_4C/graphene pellets as calculated by Archimedes principle are plotted against mixing time. Figure 5-6 shows experimentally calculated green density of compacted pallets (Green densities) and sintered densities of the composites. The values obtained after compaction were less than that of the densities calculated after sintering. The composites at different milling time show different values.

For 2 hours of milling of powder the compacted density was 2.52g/cm^3 as well as sintered density was 2.59 g/cm^3. For 3 hours of milling the green density values remains same 2.52 g/cm^3 but sintered density has a slightly low value 2.58 g/cm^3 compared with that of 2 hours milling. In comparison to 4 hours of the milling the density of sintered composite was again increased to 2.61 g/cm^3 and compacted to 2.55 g/cm^3.

By Comparison to the densities that was observed, we come to know that the density of composite after compacting(green densities) was slightly low in comparison with sintered composite, however the change of the densities are minor just change in 2nd decimal which can be negligible.

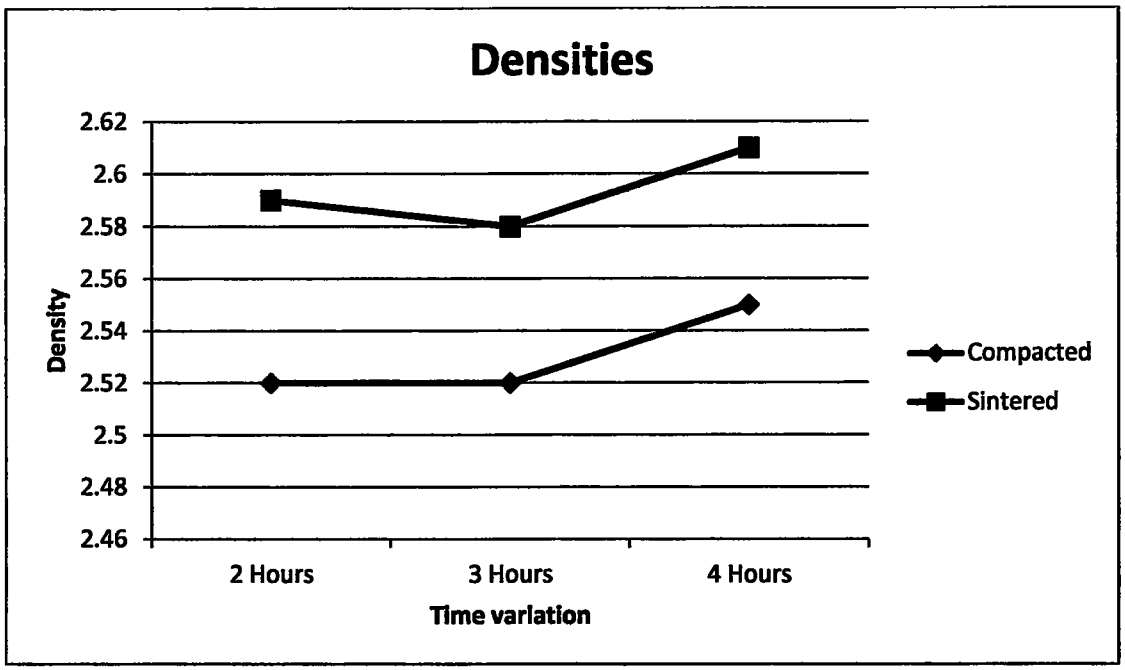

Figure 5-6: Comparison between the densities of green compacted pellets and sintered composites as function of milling time.

The increase in minor change in density with mixing time can also be explained by considering the corresponding increase in number of reinforcement particles which causes less efficient packing in the ductile aluminum matrix. The creation of more Al/B_4C

interfacial area introduces gaps between ceramic particles and metal grains, the size of B_4C fragments would be too large to fill those gaps, which may be filled by graphene. Due to the vast difference in the melting point and compressive strength of the constituents, B_4C particles act as a barrier to the rearrangement, deformation and diffusion of the aluminium particles; this may be the reason to increase the density slightly at 4 hours of milling. This will result in an overall expansion of the composite structure, thereby increasing a small amount in the density. Relatively lower density in wet mixing in the initial stages for green densities might be due to the presence of toluene.

5.5 Hardness

Figure 5-7 shows the plot for average hardness values of Al/B_4C/Graphene composite pellets for wet mixing conditions against mixing time. The values show a gradual increase with increasing mixing time. For wet mixing, average hardness observed for Al/B_4C/graphene of 60 HRB, 65 HRB and 67 HRB for 2, 3 and 4 hours in comparison with Al/B4C 51.00, 49.00 and 50.00 HRB respectively. The values show that the hardness of composite increased with increasing particle size. The presence of graphene and B_4C offers more resistance to plastic deformation which leads to increase the hardness of final composite.

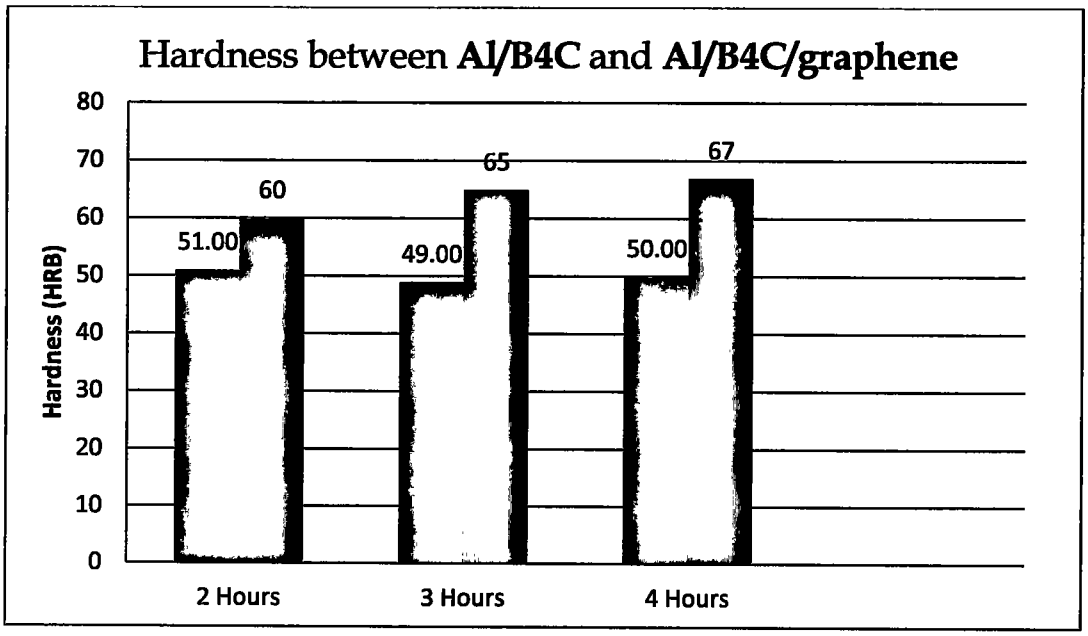

Figure 5-7: The comparison of hardness of composite under different milling time

The increase in hardness can be attributed to the increasing number of ceramic and graphene

particles and as the mixing proceeded. Particle fracture during mixing in the ball mill created more surface area; as a result the Al-B_4C-graphene interfacial area would have been increased. Aluminum is a ductile metal while boron carbide is a hard ceramic stone, while in the contrast graphene is a solid lubricant, Due to the surface incompatibility between aluminum and boron carbide particles, minute gaps between the particles were left behind, which were filled with graphene solid lubricant. For an effective load transfer to the reinforcement during mechanical loading, the bonding between matrix and reinforcement is very important, so graphene filed the minor gaps but the B_4C did not collapse with graphene and aluminium even in sintering mechanisms, because it required 2440°c temperature to melt and sintered, which is not adequate for aluminum alloy. So the hardness of the aluminium reinforced with B_4C and graphene has higher hardness in comparison with Al/B_4C composites.

Gajewska*et al.* have investigated the effect of reinforcement size on the mechanical properties of the composite and found a decrease in hardness with decreasing particle size of AlN reinforcement [60].

6. Conclusion

In summary, 6061-Al/B_4C and 6061-Al/B_4C/graphene were fabricated with powder metallurgy process. From the results following conclusion can be drawn.

- Graphene were obtained from modified Hummer's method. SEM micrographs show the nano platelets which were folded, edged and entangled.
- Raman spectroscopy analysis and XRD analysis indicates that, almost all oxygen present in graphene oxide was removed and it was converted into graphene.
- From SEM analysis it was found that the particles are more uniformly distributed in Al/B_4C/graphene composite in comparison with Al/B_4C composites.
- For two hours of milling the agglomeration was present due to the stuck of the B_4C and graphene in the aluminium matrix.Surface incompatibility between aluminium and B_4C particles and increase in interfacial area due to increased particle fragmentation with mixing time are the possible causes for degradation of hardness and density.
- Uniform distribution depends upon good mixing and milling that was obtained at 4 hours of ball milling.
- XRD studies validate the presence of B_4C and graphene in composites in solidified microstructure.
- Hardness of the composite was increased in 6061-Al/B_4C/graphene composite at 4 hours of milling, than that for the 6061-Al/B_4C composites, due to mismatch incompatibility between aluminium matrix and B_4C.
- The densities of the 6061-Al/B_4C/graphene composites were observed to 2.59, 2.56, and 2.57 for 2 hours, 3 hours and 4 hours respectively.
- The primary objective low density and high hardness has been obtained with the addition of graphene in Al/B_4C composites.
- This work is the preliminary study; detailed study is required to evaluate the contribution of graphene on mechanical properties (tensile strength etc.) of Al6061/B_4C/graphene hybrid composites.

Bibliography

[1] Mallick, P.K. Fiber-Reinforced Composites. 3rd CRC Press, 2008. Print. 2 Dec 2009.

[2] Metal Matrix Composites (Online)
https://en.wikipedia.org/wiki/Metal_matrix_composite.

[3] Thwe M.M, Liao. K (2003) Comp. Sci. Tech,, 63 ,375

[4] Basics of Metal Matrix Composites - Wiley-VCH,by KU Kainer - 2006.

[5] Esawi AMK, Borady El MA. Carbon nanotube-reinforced aluminium strips.Compos SciTechnol 2008;68(2):486–92.

[6] Liu C.B., Wang K., Luo S.L., Tang Y.H., Chen L.Y., Small 7 (2011) 1203–1206

[7] HUNT M. in "Materials EngineeringlD , Jan. 1989.

[8] Alizadeh A., Taheri-Nassaj E., Hajizamani M., J. Mater. Sci. Technol. 27 (2011) 1113e1119.

[9] Vogelsang M., Arsenault R. J. and Fisher R. M., "In-situ HVEM study of dislocation generation at Al/SiC interfaces", Metall. Trans. A, 1986, 17, 379.

[10] Sato A. and Mehrabian R., "Aluminium matrix composites: fabrication and properties"

[11] Pai B. C., Ray S., Prabhakar, K. V. and Rohatgi P. K., "Fabrication of aluminium(magnesia) particulate composites in foundries using magnesium additions to the melts", Mater. Sci. Engng, 1976,24,31.

[12] Bolotin K.I., Sikes K.J., Jiang Z., Klima M., Fudenberg G., Hone J., Kim P., Solid State Commun. 146 (2008)
351–355.

[13] Hartaj Singh, Sarabjit, Nrip Jit, Anand K Tyagi; Journal of Engineering Research and Studies, An Overview of Metal Matrix composites processing and SiC based Mechanical properties: E-ISSN0976-7916.

[14] Iijima S., Helical microtubules of graphitic carbon, Nature 354 (1991) 56–58.

[15] Geim A. K. & Novoselov K. S. Nature Materials, Vol 6 183 - 191 (2007).

[16] Fukuda H., Kondoh K., Umeda J., Fugetsu B., Fabrication of magnesium basedcomposites reinforced with carbon nanotubes having superior mechanicalproperties, Mater. Chem. Phys. 127 (2011) 451–458.

[17] Sun. F, Shi. C. Rhee. K.Y, Zhao.N, In situ synthesis of CNTs in Mg powder at lowtemperature for fabricating reinforced Mg composites, J. Alloy. Compd. 551(2013) 496–501

[18] Jia. K, Jiang, CC LK, Li WS. Improvement of interface and mechanical properties in

carbon nanotube reinforced Cu–Cr matrix composites. Mater Des 2013;45:407–11

[19] MasoudAlizadeh, TouradjEbadzadeh, Amir hosseinPakseresht, Ali Rahbari Ehsan Ghasali, "Investigation on microstructural and mechanical properties of B_4C–aluminum matrix composites prepared by microwave sintering," Journal ofMaterials Research and Technology, February 2015.

[20]Niranjan. H.B, Satyanarayana K.G, Manjunatha.B, "Effect of mechanical and thermal loading on boron carbide particles," Materials Science & Engineering A, no. 632, pp. 147-155, February 2015.

[21] Zahid. G. H, Rafi-ud-Din, Ahmad. E, Mehmood. M, Badshah S, Asghar. Z, "Effect of degassing parameters on sinterability of Al/B_4C," Powder Metallurgy, April 2014.

[22] MohdReusmaazranYusof, Azali Muhammad, NadiraKamarudin, Wilfred Sylvester Paulus, RoslindaShamsudin, Nasrat Hannah Shudin, Nurazila Mat ZaliYusof Abdullah, "Al/B_4C Composites with 5 And 10 wt% Reinforcement

[23] Akhlaghi. F, Khakbiz. M. "Synthesis and structural characterization of Al–B_4C nano-composite powders," Journal of Alloys and Compounds, no. 479, pp. 334-341, December 2008.

[24] Balasubramaniana. K, Seshadri. S.K, Mohantya. R.M, "Boron carbide-reinforced alumnium 1100 matrix composites," Materials Science and Engineering A, no. 498, pp. 42-52, November 2007.

[25] Jia-Jun Gu, Jun-Liang Liu, Di Zhang Cun-Zhu Nie, "Production of Boron Carbide Reinforced 2024 Aluminum Matrix," Materials Transactions, vol. 48, no. 5, pp. 990-995, February 2007.

[26] Mohammad Sharifi.E, Karimzadeh.F, Wear behavior of aluminum matrix hybrid nanocomposites fabricated by powder metallurgy.Volume 271, Issues 7–8, 18 July 2011, Pages 1072–1079

[27] Alizadeh A, Taheri-Nassaj E, Bharvandi HR, Preparation and investigation of Al–4 wt % B_4C nanocomposite powders using mechanical milling, pp 1039-1048

[28] Kerti I, Toptan F. Microstructural variations in cast B4C-reinforced aluminium matrix composites (AMCs). Mater Lett 2008; 62:1215–8

[29] Han B.Q, Lee .Z, Witkin D, Nutt. S, Lavernia E.J. Metall.Mater.Trans.A36 (2005)957–965

[30] Pierard. N, Fonseca. A, Colomer J.F, Bossuot. C, Benoit. J.M, Van Tendeloo.G, et al., Ball milling effect on the structure of single-wall carbon nanotubes, Carbon 42 (2004) 1691–1697.

[31] Awerbuch J., Goering J. and Busking K., "In Mini Mechanics Analysis and Testing of Short Fibre Composites: Experimental Methods and Results", Vol. 121, 1988.pp964 (American Society for Testing and Materials, Philadelphia. Pennsylvania).

[32] Khalid FA, Beffort O, Klotz U E, Keller B A, Gassser P, Vaucher S, Study of microstructure and interfaces in an aluminium–C60 composite material [J]. ActaMaterialia, 2003, 51(15): 4575–4582.

[33] Wang L, Choi H, Myoung JM, Lee W. Mechanical alloying of multi-walledcarbon nanotubes and aluminum powders for the preparation of carbon/metalcomposites. Carbon 2009;47:3430–3.

[34] Hall E.O, Proc.Phys.Soc.B64(1951)747–753.

[35] Miracle. D.B, Compos. Sci. Technol. 65, 2526 (2005)

[36] Chawla. K.K, Chawla N, Metal–Matrix Composites (Springer, New York, 2006), pp. 166–195

[37] Zhang D.L., Prog. Mater.Sci. 49, 537 (2004).

[38] DieterG.E., Mechanical metallurgy, 3rd edi., McGraw-Hill, 1976.

[39] Kennedy. A.R, "The microstructure and mechanical properties of Al-Si-B_4C metal matrix composites", Journal of materials Science 37 (2002) 317-323.

[40] Inam, H. Yan, M. J. Reece and T. Peijs: Adv. Appl. Ceram., 2010, 109, (4), 240–245.

[41] Suresha, S., Sridhara, B.K., 2010, "Effect of addition of graphite particulates on the wear behaviour in Aluminum–silicon carbide–graphite composites", Materials and Design, 31, 1804–1812.

[42] Hashim J, Looney L, Hashmi MSJ. Metal matrix composites: production by the stir casting method. J Mater Process Technol 1999;92–93:1–7.

[43] Baradeswaran A, Elayaperumal A. Influence of B4C on the tribological and mechanical properties of Al 7075–B4C composites. Composites: Part B 2013;54:146–52.

[44] WIKIPEDIA (2005). Turbo molecular pump [Online]. Available at http://en.wikipedia.org/wiki/Turbomolecular_pump (accessed 1 Feb 2005).

[45] FEI. The Quanta 200 User's Operation Manual 2nd ed. (2004).

[46] JEOL. Guide to scanning electron Microscopy [Online]. Available http://www.jeol.com/sem/docs/sem_guide/tbcontd.html (accessed 1 Feb 2005).

[47] XRD basics. [Online]. Available at https://en.wikipedia.org/wiki/XRD

[48] Material research laboratory [Online] http://www.mrl.ucsb.edu/centralfacilities/x-ray/basics

[49] Tuinstra. F, and Koenig .J, Chem. J, Phys. 53, 1126 (1970).

[50] Nemanich .R. J, and Solin. S. A, Phys. Rev. B 20, 392 (1979).

[51] Cancado. L. G. et al., Phys. Rev. Lett. 93, 047403 (2004).

[52] Novoselov. K.S, Geim.A.K, Morozov.S.V, Jiang. D, Zhang Y, DubonosS.V, Grigorieva. I.V, Firsov, A.A, Science 306 (2004) 666

[53] Ferrari. A.C, Robertson. J (Eds.), Raman spectroscopy in carbons: From nanotubes to diamond. Philos. Trans. R. Soc. Ser. A 362, 2267–2565

[54] Material research laboratory [Online], Available at http://www.mrl.ucsb.edu/centralfacilities/x-ray/basics

[55] Tuinstra. F, and Koenig. J, J. Chem. Phys. 53, 1126 (1970).

[56] Nemanich. R. J, and Solin. S. A, Phys. Rev. B 20, 392 (1979).

[57] Ferrari, A. C. Solid State Commun. 2007, 143, 47-57.

[58] Perez-Btanmante. R et al. / Journal of Alloys and Compounds 615 (2014) s578-s582.

[59] Sharifi, M.E., Karimzadeh, F. and Enayati, M.H. (2011). Fabrication and evaluation of mechanical and tribology properties of boron carbide reinforced aluminium matrix nanocomposites. Materials and Design 32: 63-71.

[60] Jan Dutkiewicz, Jerzy Morgiel Marta Gajewska, "Effect of reinforcement particle size on microstructure and mechanical properties of AlZnMgCu/AlN nano-composites produced using mechanical alloying," Journal of Alloys andCompounds, vol. 586, no. 1, pp. 423-427, 2012.

Vita

Abdul Malik, the author of this thesis was born on February 26, 1989 in Fateh Jang (Attock). He passed Matric examination from Govt. Boys High School No.1 Fateh Jang in 2006. After that, he got admission in Government Post Graduate College Asghar Mall Rawalpindi and passed his F.Sc (Pre-engineering) in 2009 and graduation (B.Sc. in Physics) from same college in 2010. Further for Master Degree (MSc Physics) took admission in University of Wah, Wah Cant and completed in 2012. For higher education, he took admission in International Islamic University Islamabad Fall 2013 for M.S Physics.